Journal of Glaciology

Morphological diversity of microalgae and Cyanobacteria of cryoconite holes in Northern Victoria Land, Antarctica

Flavia Dory[1], Veronica Nava[1], Linda Nedbalovà[2], Valentina Soler[1], Biagio Di Mauro[3], Giacomo Traversa[3], Morena Spreafico[1] and Barbara Leoni[1]

[1]Department of Earth and Environmental Sciences, University of Milano-Bicocca, Milan, Italy; [2]Department of Ecology, Faculty of Science, Charles University, Prague 2, Czech Republic and [3]National Research Council of Italy, Institute of Polar Sciences, Via Cozzi 53, Milan, Italy

Article

Cite this article: Dory F, Nava V, Nedbalovà L, Soler V, Di Mauro B, Traversa G, Spreafico M, Leoni B (2025) Morphological diversity of microalgae and Cyanobacteria of cryoconite holes in Northern Victoria Land, Antarctica. *Journal of Glaciology* **71**, e37, 1–22. https://doi.org/10.1017/jog.2025.12

Received: 5 August 2024
Revised: 23 January 2025
Accepted: 12 February 2025

Keywords:
Antarctica; biodiversity; cryoconite holes; Cyanobacteria; glaciers; microalgae

Corresponding author: Flavia Dory; Email: flavia.dory@unimib.it

Abstract

Cryoconite holes are supraglacial depressions containing water and microbe-mineral aggregates. Their autotrophic component plays a central role in reducing the albedo of glaciers and could contribute to sustaining the cryoconite food web. However, knowledge of its diversity is still limited, especially in Antarctica. Moreover, the study of cryoconite microalgae is challenging due to the limitations of molecular approaches, such as incomplete genetic databases and the semiquantitative nature of the data. Furthermore, it is equally difficult to examine the development of microalgae in sediment by using standard counting methods for water-living organisms. By using an adaptation of the high-speed density gradient centrifugation method, we provide a comprehensive description of the phenotypic characteristics, abundance and community structure of microalgae and Cyanobacteria in different cryoconite holes located in different glaciers of Northern Victoria Land, East Antarctica. We described 36 morphotypes belonging to Cyanobacteria, green algae and diatoms, revealing that cryoconite holes encompass a remarkably high diversity of photoautotrophs. The adapted protocol enabled the application of a standard microscopic approach, which provided crucial and comparable information on morphological characteristics, biovolume and community organization from a unique environment. The study poses the basis for the taxonomy of photoautotrophs as well as their diversity and distribution in cryoconite habitats.

1. Introduction

The cryosphere covers about one-fifth of the Earth's surface, sustaining a surprising abundance of life above, within, and below the ice (Boetius and others, 2015). On the surface of glaciers and ice sheets, particular hotspots of biodiversity occur in cryoconite holes, small depressions (from millimeters to tens of centimeters) in the ice surface filled by water and sediment at the hole base. The term 'cryoconite' has been used to describe granular sediment in the ice surface comprising both mineral and biological material (Cook and others, 2016). Cryoconite holes form when dark material (e.g. soil or dust) is deposited onto the glacier's surface. They can cover a large portion of a glacier, with percent cover ranging from 0.002% to 8.6% (Hells Gate Ice Shelf, Antarctica) (Traversa and others, 2024) and values of cover up to 16% in several other areas (Hodson and others, 2013), and are now recognized as an important microbial habitat and a major component of supraglacial ecosystems (Anesio and Laybourn-Parry, 2012).

Cryoconite biota may be delivered to glacier surfaces directly from the atmosphere *via* both wet and dry deposition, and only cryo-tolerant species survive (Cook and others, 2016; Rozwalak, 2022). Because cryoconite sediment has low albedo relative to the surrounding ice, it efficiently absorbs solar radiation, causing an acceleration of the melting of ice beneath accumulations of cryoconite sediment (Cameron and others, 2012; Di Mauro, 2017). This reduction in albedo may result mainly from abiotic factors (for example humic substances and mineral particles) but also from biological components, such as algae, that have been shown to play a determining role through their pigmentation (Di Mauro, 2020; Hotaling, 2021). In glaciers, snow and ice algae pigments have been shown to reduce albedo by as much as 48% and 56%, respectively, when compared to a 'clean' surface (Bøggild and others, 2010; Di Mauro, 2024). Cryoconite holes, even if they can cover a large portion of a glacier, have lower effects on glacier-wide albedo compared to snow and ice algae and dispersed sediment, as they are narrow and vertical, and thus only receive direct radiation for short periods (Bøggild and others, 2010; Traversa and others, 2024). However, warm conditions are able to collapse cryoconite holes by melting the ice surface faster than the solar-heated cryoconite, thus deepening the hole and re-dispersing cryoconite sediment onto the ice surface (Takeuchi, 2018).

https://doi.org/10.1017/jog.2025.12 Published online by Cambridge University Press

Previous studies have demonstrated that cryoconite communities tend to be dominated by Proteobacteria, Bacteroidetes, Cyanobacteria, and microalgae (Cameron and others, 2012; Edwards, 2013; Sommers, 2018). Notably, filamentous phototrophic Cyanobacteria and coccal heterotrophic bacteria have been demonstrated to act as cryoconite 'engineers', forming discrete dark granules up to 3 mm in diameter (Takeuchi and others, 2001; Langford and others, 2010). These granules act as a substrate for the growth of bacteria, microalgae, and protozoa (Mueller and others, 2001; Christner and others, 2003; Cameron and others, 2012). Phototrophic microalgae also play a crucial role in sustaining the entire food web in cryoconites, as these primary producers convert atmospheric CO_2 into organic matter, which acts as a substrate for heterotrophs. Among the primary producers, Cyanobacteria frequently dominate both biomass and C fixation in cryoconite holes (Cook and others, 2016). In addition, Cyanobacteria in cryoconite holes in Antarctica have been shown to play an important role in nitrogen cycling, as they fix nitrogen and provide key nutrients to other cryoconite microbiota (Tranter, 2004). Despite the essential ecological role of cryoconite primary producers, the diversity, composition, and morphological features of these organisms in glacial habitats remain poorly understood.

Much of the current knowledge about cryoconite has come from works in the Arctic; for example, in the recent list of taxa reported from cryoconite holes, 60% are known from polar glaciers in the Arctic while only 43% are known from Antarctic regions (Kaczmarek and others, 2016). However, several studies found a contrasting biota between Antarctic and Arctic cryoconites (Millar and others, 2021), probably explained by the geographic isolation of the Antarctic continent and by extreme hydrochemical conditions within cryoconite holes that are unique to Antarctica (Tranter, 2004; Hodson, 2008). These conditions could result from continuous periods of isolation from atmospheric exchange (of up to 11 years) that have been observed in the Antarctic (Fountain and others, 2004; Tranter, 2004; Bagshaw and others, 2007). In addition, a recent study showed that both biological and biochemical parameters among the different zones of an Antarctic glacier are characterized by a certain complexity and heterogeneity caused by local factors (depth of cryoconite holes, diameter, organic matter, total carbon, particle size, and mineral diversity), local inoculation sources, and long-range atmospheric transport mechanisms (Weisleitner and others, 2020). Thus, there is a lack of studies on cryoconite microalgae in the Antarctic, even though they can participate in the reduction of ice albedo (Traversa and others, 2024), and phototrophic processes are complex and expected to increase in the future (Cook and others, 2016). Indeed, prolonged ablation season caused by climate change will likely extend the growing periods for photoautotrophs, which in turn will potentially boost cryoconite granule formation and surface algae proliferation, further reducing ice surface albedo (Hodson, 2007, 2010). This impact of algae blooms on snow melt and its associated indirect feedback effects, conceptualized by the term 'bio-albedo feedback', can largely accelerate the effects of warming, with severe repercussions on the global carbon cycle (Cook and others, 2017). For example, warming was estimated to strengthen net autotrophy and increase atmospheric C fixation on the Greenland ice sheet (Cook, 2012).

Studies addressing the diversity of Antarctic microalgae based on morphological features are scarce; the only group that makes an exception to this rule is diatoms, which have long been studied in the Antarctic region based on morphological diagnostics and are well-described (Sabbe and others, 2003). A broad taxonomic revision of Antarctic diatoms conducted over the last 20 years has thus revealed a unique flora with a high degree of endemism, with, in some areas of Antarctica, at least 40 percent of the species being endemic (Vyverman, 2010). Other than this, most of the studies that have addressed the diversity of Antarctic microalgae have used molecular methods, with a particular focus on Cyanobacteria (Zhang and others, 2015; Jungblut, 2016; Lizieri and others, 2022). The information provided by molecular approaches, despite helping species identification and unraveling cryptic diversity, is limited by the incompleteness of genetic databases and the semiquantitative nature of data and is dependent on isolation and cultivation processes (Borics and others, 2021). Numerous photoautotrophs from these extreme environments are not easily cultivable in controlled conditions (Procházková and others, 2021), implying that individuals that cannot be cultivated are largely undervalued. In addition, molecular tools provide limited information on abundance and community structure, making these parameters difficult to compare with other environments. Unlike molecular methods, morphological feature identification (such as filamentous, colonial, or unicellular forms, color, or presence of heterocysts) allows for highlighting consistent features and common characteristics among identified species. It provides valuable information relative to the bio-albedo effect, the ecological dynamics of these microorganisms, and the habitat characteristics (Lizieri and others, 2022), which is especially important in the understudied Antarctic cryoconite holes (Wejnerowski, 2023).

With the intent to fill these existing gaps, this study presents the morphological descriptions of Cyanobacteria and microalgae taxa obtained from cryoconite holes sampled across four glacial locations in Northern Victoria Land, East Antarctica. By providing a highly comprehensive description of the diversity of primary producers in cryoconite holes, this study aims to (1) assess how much the community of primary producers changes (in terms of diversity and composition) within and among different glaciers, (2) broaden the list of organisms living in cryoconite holes by coupling their description at the most detailed taxonomic level with the characterization of their morphological features.

Ultimately, the knowledge gained in this study should contribute to a better understanding of the ecological role of primary producers within the food web of cryoconite habitats and their capacity to reduce the ice albedo in Antarctic glaciers. This study will also lay the basis for future investigation of the photoautotroph taxonomy in extreme environments. Furthermore, this work will yield a wealth of information on Antarctica's biodiversity, which is urgent to assess before rapidly escalating human activity and changing environmental conditions. This is particularly important in order to identify rare or endemic glacial species that could be endangered as a result of climate change, as well as species that could serve as a source of organisms for the emergent ice-free area.

2. Materials and methods

2.1. Sampling

Samples of cryoconite from 26 individual holes were collected in the Northern Victoria Land in Antarctica between November 2022 and January 2023. Four separate glacial locations were sampled: Hells Gate Ice Shelf, Priestley Glacier, Nansen Ice Shelf—Tarn Flat area (hereafter reported as Tarn Flat), and Nansen Ice Shelf—median area (hereafter reported as Nansen) (Fig. 1). Priestley was the most distant location from the others, namely about 46 km from Hells Gate, 49 km from Nansen, and 61 km from Tarn Flat. Hells Gate was about 15 km distant from Nansen and

https://doi.org/10.1017/jog.2025.12 Published online by Cambridge University Press

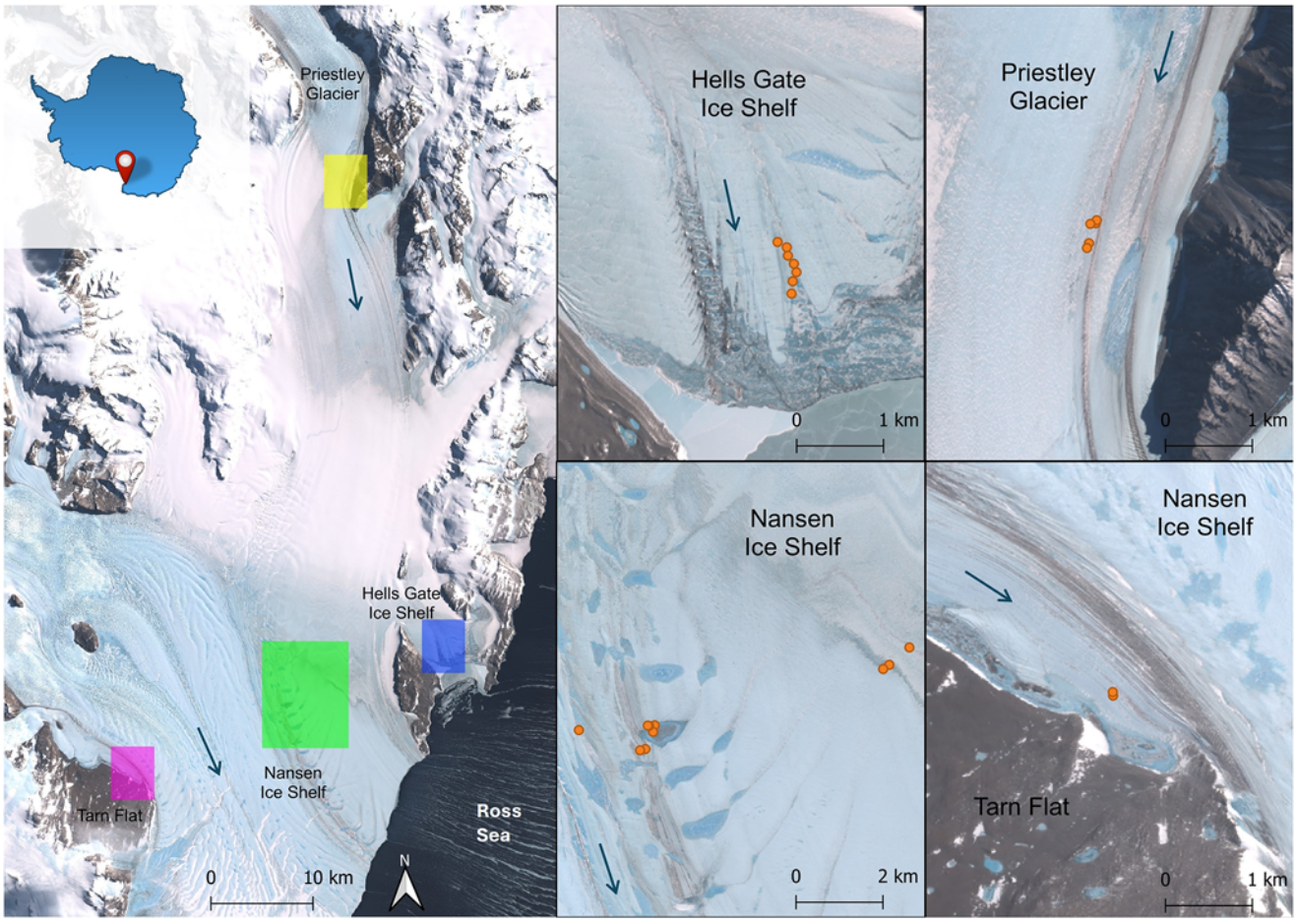

Figure 1. Northern Victoria Land (East Antarctica) and locations of the four glacial areas. in each glacial area, orange points correspond to the sampled cryoconite holes. Blue arrows represent the direction of the glacier flow. Satellite images from Google Earth.

about 33 km distant from Tarn Flat, and the Nansen and Tarn Flat were separated by about 18 km. The distribution of the cryoconite on the sampled area averaged 4 cryoconite holes every 100 m^2, with maximum peaks in certain areas of 84 cryoconite holes every 100 m^2 (Traversa and others, 2024). An example of the cryoconite cover on the glacial area is shown in the different pictures in Fig. S1. The sampled cryoconites differed in the presence or absence of lids, the dimension (from 10 to 300 cm of diameter, with an average of 70 $\pm$ 13 cm), and their depth (from 5 to 50 cm). The details of each sample and its associated coordinates are reported in Table S1. Within each glacier, cryoconite samples were collected from a distance of about 40 m (Tarn Flat samples), 300 m (Priestley samples), 600 m (Hells Gate samples), and 7 km (Nansen samples) from each other. Cryoconite samples were collected using sterile spoons, stored in sterile 50 mL Falcon tubes and immediately frozen (−20°C) for transportation to Italy. At the laboratory, samples were kept frozen at −20°C, following the sampling procedure for glacial algae (Di Mauro, 2020). Abiotic parameters (water temperature, electrical conductivity, pH, and dissolved oxygen) were measured *in situ* at least in one cryoconite hole from each glacial location using a multiparametric probe (HANNA-HI98194). The water temperature in the cryoconite holes ranged between 0.0 and 0.7°C (average 0.25 $\pm$ 0.07°C) and the mean pH was 6.9 $\pm$ 0.13 (Figure S2). Electrical conductivity averaged 218.7 $\pm$ 52.8 $\mu S\ cm^{-1}$ and the mean value of dissolved oxygen was 14.0 $\pm$ 0.4 ppm.

For each glacial location, pictures at different magnifications were used to characterize the cryoconite sediment (Fig. 2). In Hells Gate, the cryoconite tone was dark, and both granular and loose material were detected. Granules were mainly oval. In Priestley Glacier, cryoconite was in the form of sand, light, and brownish. In Tarn Flat, the cryoconite tone was light-colored, and small granules with irregular surfaces were detected. In the Nansen location, cryoconite was composed of diverse mineral irregular grains.

2.2. Microalgae and Cyanobacteria separation from sediment

For morphological identification, cryoconite samples were thawed and homogenized for 10 min. Then, subsamples of 10 mL were transferred into pre-weighted sterile 50 mL Falcon tubes. Purification through high-speed density gradient centrifugation was performed by the use of Nycodenz as a density gradient medium (density 1.31 $g\ mL^{-1}$), adapting the protocol of Amalfitano and Fazi (2008) for microalgae samples. Thus, 10 mL of Nycodenz was carefully placed at the bottom of the Falcon tube beneath the cryoconite sediment, using a Pasteur pipette with adequate length to reach the bottom of the tube (Fig. 3). All tubes were centrifuged (10 000 rpm) for 60 min at 4°C. After the centrifugation, four distinct layers were clearly visible (from bottom to top): (1)

https://doi.org/10.1017/jog.2025.12 Published online by Cambridge University Press

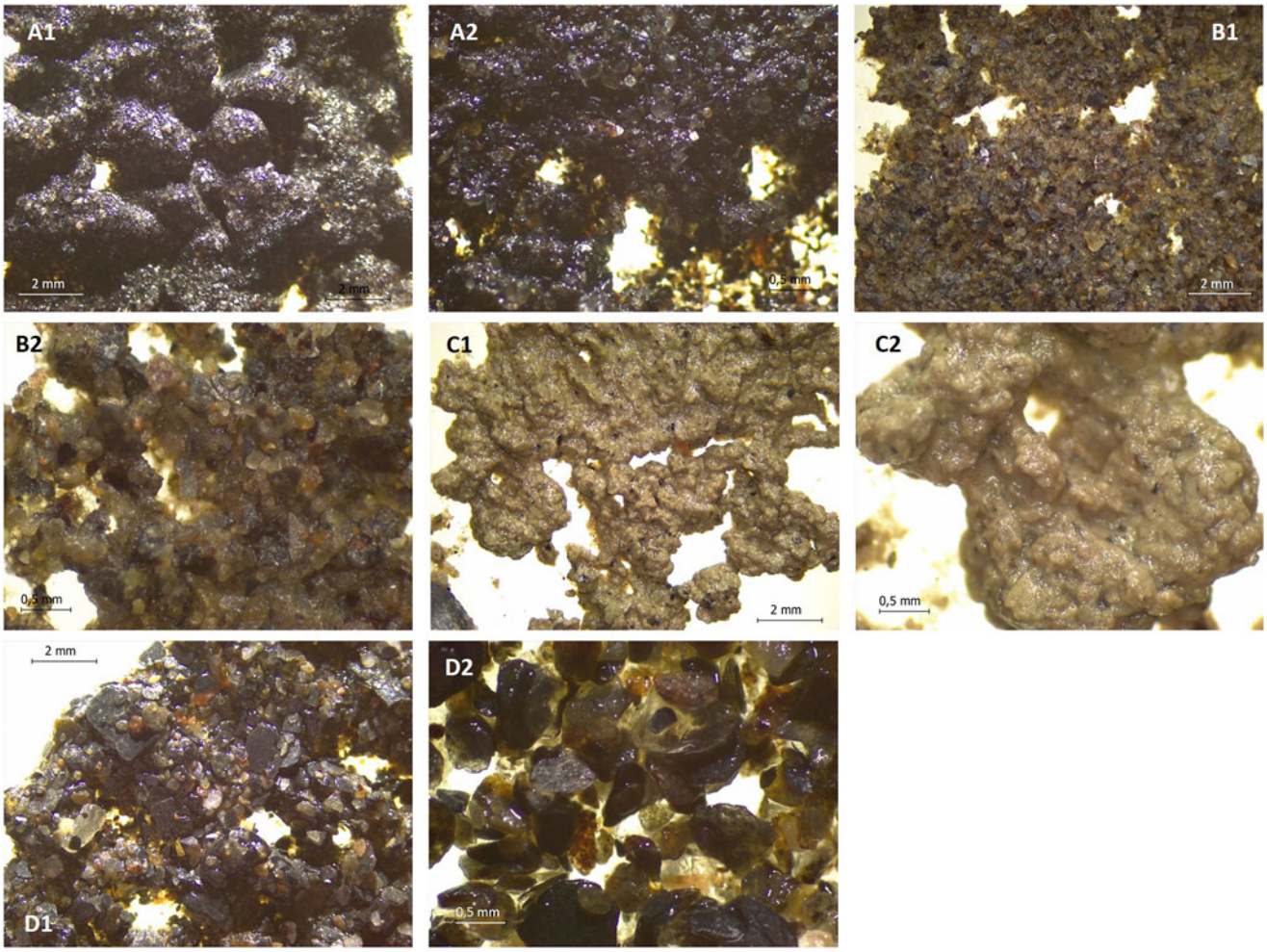

Figure 2. Description of cryoconite from each glacial location, at ×8 and ×25 magnifications. (A) Hells gate; (B) Priestley; (C) Tarn Flat and (D) Nansen.

sediment pellet, (2) Nycodenz, (3) cell layer, (4) supernatant. The layer containing microalgae and Cyanobacteria was then collected using a Pasteur pipette, transferred into sterile 15 mL Falcon tubes, and frozen (−20°C) until microscopic identification and counting. The remaining cryoconite sediment pellet was rinsed three times with distilled water, dried at 60°C, and weighed to calculate the biovolume of taxa by dry weight of sediment.

2.3. Sample preparation, measurements and biovolume calculation

Algae counting was performed at 400× magnification under an IM35 inverted microscope, following the Utermöhl (1958) method. Identification of Cyanobacteria and green algae was based on the microscopic analysis of their morphological features, according to specific identification keys (Ettl and Gärtner, 1999; Komárek and Anagnostidis, 2005; Hindák, 2008; Rosen and Amand, 2015; Nienaber and Steinitz-Kannan, 2018), allowing to identify the taxa at the genus level and species level when possible. In addition, for a given taxon, we distinguished between different morphotypes, i.e., differences in pigmentation, morphology, or size. Filamentous taxa were counted at the trichome (50 μm) level, as cells were not always distinguishable.

Concerning diatom identification, permanent slides were prepared using standard procedures: samples were heated with 30% hydrogen peroxide (H_2O_2) for a minimum of 4 h in order to oxidize organic material. Then, carbonates were removed by adding concentrated hydrochloric acid (HCl, 1 M); and the processed material was then rinsed with distilled water in four centrifugation steps (Battarbee, 2001). Cleaned material was transferred on a 24 × 24 mm coverslip and the slides were mounted using a drop of Naphrax (R.I. = 1.7). Diatoms were identified using an optical microscope at 1000× magnification under oil immersion. Identification of diatom species was based on the microscopic analysis of their morphological features, according to specific identification keys (Lange-Bertalot and others, 2017), updated to recent specific taxonomic literature (Kopalová and others, 2011; Van de Vijver and others, 2011, 2016; Zidarova and others, 2016a, 2020).

Cell biovolume was estimated by assimilating each taxon to a simple geometric form, according to the literature (Druart and Rimet, 2008; Laplace-Treyture and others, 2021). When it was possible, a number of 30 specimens were measured according to the European standard, to calculate a mean cell biovolume (μm^3); however, due to the small size of the population, at least 10 individuals were measured for low-abundant specimens. The final biovolume was obtained by multiplying the mean cell biovolume of each taxon by the dry weight of sediment and expressed in $\mu m^3\ g^{-1}$.

https://doi.org/10.1017/jog.2025.12 Published online by Cambridge University Press

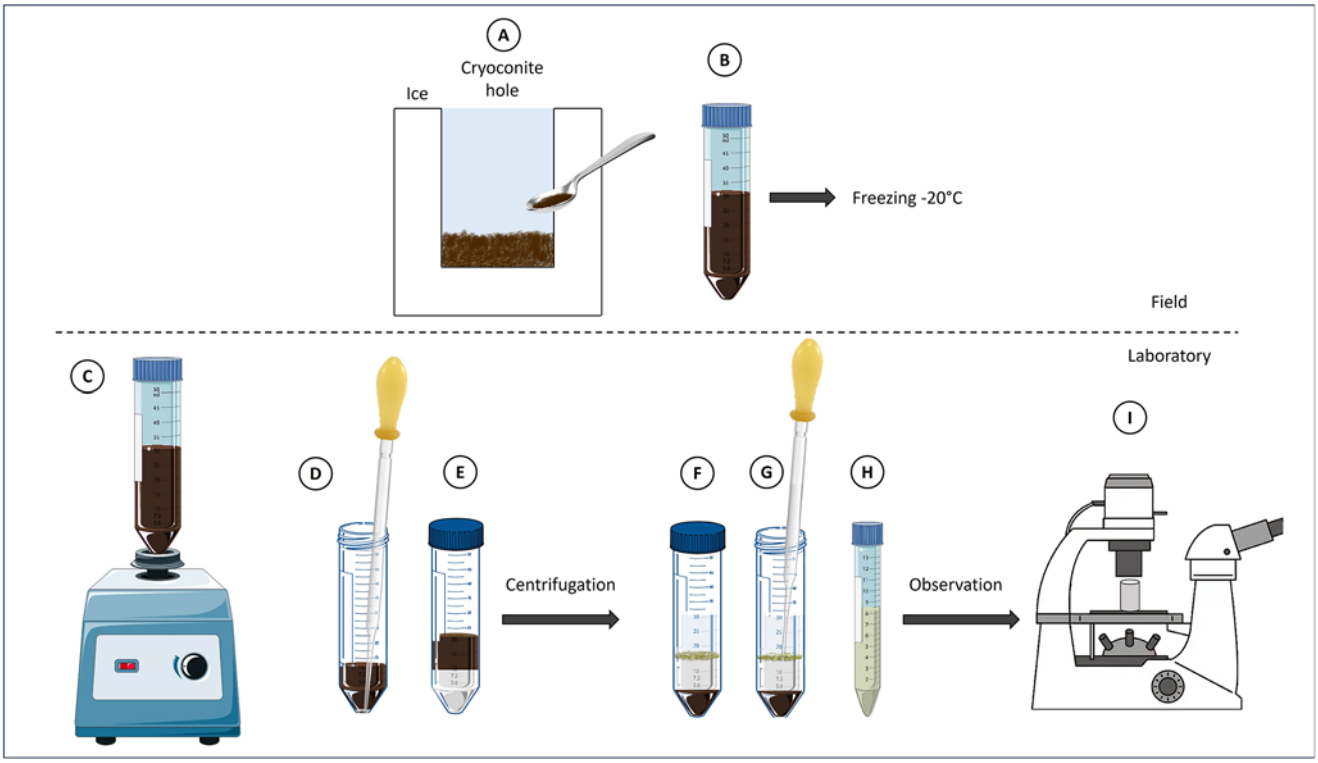

Figure 3. Schematic representation of the microalgae isolation from cryoconite samples using the purification through high-speed density gradient centrifugation method. Cryoconite sediment was sampled from cryoconite hole (A) and then stored in sterile 50 mL Falcon tubes at −20°C (B). At the laboratory, cryoconite samples were thawed and mixed for 10 min (C). Subsamples of 10 mL were placed in sterile 50 mL Falcon tubes and Nycodenz (density 1.3 g mL^{-1}) was carefully placed beneath the sediment using a Pasteur pipette (D). It resulted in two layers (from bottom to top: 1. Nycodenz and 2. Cryoconite sediment) (E). All tubes were centrifuged (10 000 rpm) for 60 min at 4°C. After the centrifugation, four distinct layers (bottom to top, 1. Sediment pellet, 2. Nycodenz, 3. Cell layer, 4. Supernatant) were clearly visible (F). The cell layer containing microalgae was then collected using a Pasteur pipette (G), transferred into sterile 15 mL Falcon tubes (H), and Frozen (−20°C) until microscopic identification (I).

2.4. Statistical analyses

The Shannon diversity index and the richness (number of genera) were calculated at the genus level with the *vegan* package in R (Oksanen, 2010). Similarity percentage (SIMPER) analyses (Clarke and Warwick, 1994) were performed to estimate the percentage contribution of the main taxonomic groups in the cryoconite holes. To test possible variations in biovolume or community structure among the holes within a glacier, we performed a Levene's test (for algal biovolume) and its multivariate analog (Betadisper test) for community composition. The difference in photoautotroph biovolume, Shannon diversity, and richness between the four different locations was assessed by using a one-way analysis of variance followed by post-hoc tests. The pairwise comparisons were performed using Tukey HSD method. Variation in the community composition was analyzed by nonmetric multidimensional scaling (NMDS). The NMDS analysis was based on Bray-Curtis dissimilarity matrices (Legendre and Legendre, 1998) calculated from the biovolume of taxa at the genus level. The NMDS was performed by using the metaMDS procedure in the R package *vegan*, which uses adequate dissimilarity measures, runs NMDS repeatedly with random starting configurations, compares results, and stops after finding a similar minimal stress solution twice (Oksanen, 2010). Additionally, we used permutational analysis of variance (PERMANOVA) using the adonis function in the R package *vegan* to test a possible effect of the location on community composition. The difference in temperature, electrical conductivity, dissolved oxygen, and pH among the four glacial locations was assessed by using a one-way analysis of variance. Regarding the absence of significant differences in the abiotic parameters among the locations, we did not report the data in the Results section. Ranges of abiotic parameters for the four glacial locations are reported in Fig. S2. All the statistical analyses were processed using R software (R Development Core Team, 2018).

3. Results

3.1. Distribution of the taxa

The description of the diversity and composition of Cyanobacteria and microalgae assemblages in cryoconite holes allowed the identification of 36 morphotypes belonging to Cyanobacteria, green algae, and diatoms. A major part of the taxa, i.e. 12 morphotypes of 36, were observed in only one sample (Fig. 4). Among these taxa, only one specimen was counted for *Cymbella* sp. and *Stigonema minutum*, while for all other morphotypes, several specimens were counted within the same sample. Nine morphotypes were observed in less than five samples and eight others between five and ten samples. Seven morphotypes were counted in more than 10 samples, including the cyst stages of *Sanguina* sp., *Luticola gaussii, Pseudanabaena* sp., and the *Oscillatoria* sp. Mph 4.

The photoautotroph biovolume and Shannon diversity did not differ significantly within each glacial location (p-value = 0.8 and p-value = 0.4, respectively). However, the photoautotroph biovolume was significantly different according to the location (F = 5.1, p-value = 0.007) (Fig. 5A and B). The total biovolume was higher

https://doi.org/10.1017/jog.2025.12 Published online by Cambridge University Press

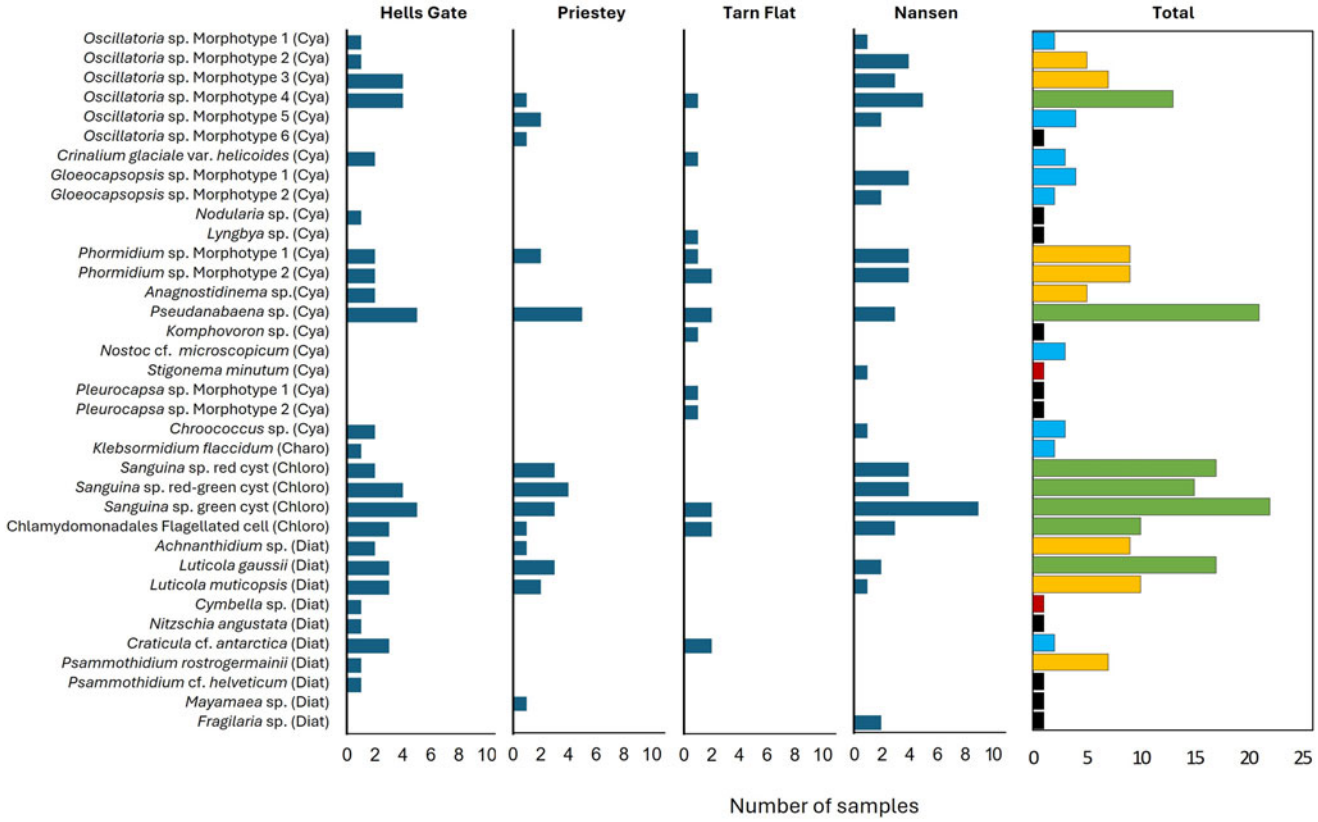

Figure 4. Frequency of occurrence of taxa in the studied samples. The colors refer to the level of occurrence: Red and black for taxa observed in only one sample, as a unique specimen (red) or several times (black); blue for taxa observed in ≤5 samples; yellow for taxa observed in >5 and ≤10 samples; green for taxa observed in more than 10 samples. Cya: Cyanobacteria; Diat: Diatoms; Chloro: Chlorophytes; Charo: Charophytes.

in the Hells Gate samples (2865 ± 988 μm^3 g^{-1}). The total biovolume was also high in the Priestley location (852 ± 534 μm^3 g^{-1}). Finally, the photoautotroph biovolume was lower in the Tarn Flat (126 ± 82 μm^3 g^{-1}) and Nansen locations (117 ± 37 μm^3 g^{-1}). The Shannon diversity and the richness calculated on the photoautotroph genera also significantly differed among the locations ($F = 4.5$, p-value = 0.01 and $F = 5.5$, p-value = 0.005, respectively). In particular, the Shannon diversity was significantly different between Hells Gate and Nansen (p-value = 0.03) and between Hells Gate and Priestley (p-value = 0.03), and the richness of genera was significantly different between Tarn Flat and Nansen (p-value = 0.03), and between Nansen and Hells Gate (p-value = 0.01). The higher diversity and richness were found in Tarn Flat samples (1.2 ± 0.1 and 8.5 ± 2.5, respectively). Mean diversity and richness were also high in Hells Gate samples (1.1 ± 0.2 and 7.3 ± 0.4, respectively) but highly variable, with maximal values of 1.7 for Shannon diversity and 9 for richness. The lower diversity and richness were found in the Nansen and Priestley locations. The non-metric multidimensional scaling based on the microalgae and Cyanobacteria genera and the PERMANOVA showed that the community composition did not differ among the glacial locations ($F = 1.14$, p-value = 0.27).

The SIMPER analysis showed that the photoautotroph community in the cryoconite holes was dominated by Chlorophytes (45%) followed by Cyanobacteria (40.1%), Diatoms (14.6%), and Charophyta (<1%). The Oscillatoriales (Cyanobacteria), the Chlamydomonadales, and the Diatoms (especially Achnanthales, Naviculales, and Cymbellales) showed the highest biomass in the Hellsgate location (Fig. 5B). At the genus level, the dominant taxa were *Sanguina* sp. (24%), the flagellated stage of Chlamydomonadales (21%), *Oscillatoria* sp. (20%), *Phormidium* sp. (7%), *Gloeocapsopsis* sp. (6%), and *Luticola* sp. (5%).

3.2. Morphological description of the taxa

1. Cyanobacteria

Oscillatoria sp. Morphotype 1 (*Fig. 6a*) Trichome generally forms long filaments of 18 ± 4 cells per 50 μm (mean ± se), relatively straight. Cells are shorter (1.9–3.9 μm) than wide (7.4–9.9 μm), with a ratio length/width of 0.34. Trichome biovolume (for a given length of 50 μm) is high (2837 ± 606 μm^3). Cells are green to yellow–green, without visible sheath, heterocyst, or granules. End cells are attenuated and slightly capitated. Separation disks are often present.

Remarks: The shape and dimensions of Mph 1 correspond with the genus *Oscillatoria* and was present in two samples (one sample from Hells Gate, biovolume of 2300 μm^3 g^{-1}, and one from Nansen, biovolume of 49 μm^3 g^{-1}).

Oscillatoria sp. Morphotype 2 (Fig. 6b) Trichome is a straight filament, with a biovolume of 903 ± 78 μm^3 for 50 μm. Cells are shorter (1.4–2.9 μm) than wide (4.0–6.2 μm) with a ratio length/width of 0.42. The trichome counts approximately 27 ± 3 cells for 50 μm. Separation disks and sheaths are not visible. Cells are yellow to brownish, sometimes green. Pores are rarely observed

https://doi.org/10.1017/jog.2025.12 Published online by Cambridge University Press

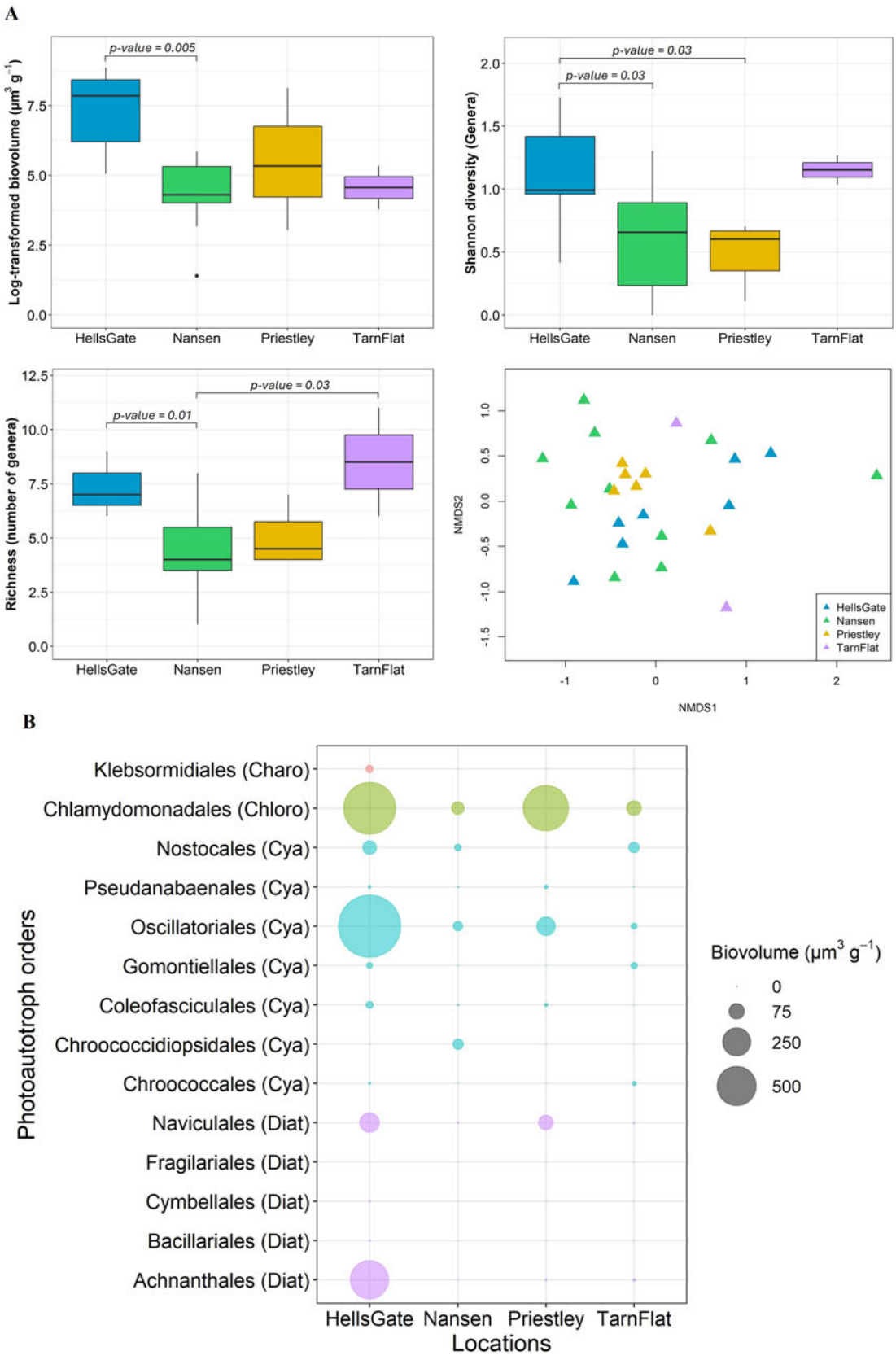

Figure 5. (A) Total photoautotroph biovolume, Shannon diversity, richness, and non-metric multidimensional scaling (NMDS) ordination of Bray-Curtis dissimilarity matrix of microalgae and Cyanobacteria genera. The stress value for the NMDS was 0.182. (B) Biovolume of the different orders of photoautotrophs in each location. Cya: Cyanobacteria; Diat: Diatoms; Chloro: Chlorophytes; Charo: Charophytes.

https://doi.org/10.1017/jog.2025.12 Published online by Cambridge University Press

Figure 6. Morphotypes in cryoconite holes in Northern Victoria Land belonging to the Cyanophyceae. (a–f) Morphospecies belonging to the Oscillatoria genus: (a) *Oscillatoria* sp. (Mph 1); (b) *Oscillatoria* sp. (Mph 2); (c) *Oscillatoria* sp. (Mph 3); (d) *Oscillatoria* sp. (Mph 4); (e) *Oscillatoria* sp. (Mph 5); (f) *Oscillatoria* sp. (Mph 6). Black scales represent 50 μm.

https://doi.org/10.1017/jog.2025.12 Published online by Cambridge University Press

but may be present in the chromoplasm. Although the apex of the trichome does not exhibit clear differentiation from its base, the terminal cell is slightly oval and attenuated.

Remarks: Mph 2 was present in five samples, mainly in the Nansen location. This morphotype was distinguished from Mph 1 by the width and a smaller biovolume.

Oscillatoria sp. Morphotype 3 (Fig. 6c) Trichome of Mph 3 is straight, with a biovolume of 1588 $\pm$ 305 μm^3 for 50 μm. Cells are shorter (1.5–5.2 μm) than wide (5.0–10 μm) with a ratio length/width of 0.48. The trichome counts approximately 18 $\pm$ 2 cells for 50 μm. Color varies from blue-green to brown, relatively dark. A lot of blue-green granules are always present, many localized in the region of the centroplasm. Terminal cells are often oval and attenuated, sometimes capitate. Separation disks are also observed. The sheath is absent. Cells are not always easily distinguishable because of the numerous granules.

Remarks: Mph 3 was observed in seven samples from Hells Gate and Nansen locations, often together with other *Oscillatoria* morphotypes. It counts among the morphotypes characterized by the higher biovolume. The morphotype is distinct from the others by the numerous granules and the width, higher than Mph 2 but smaller than Mph 1.

Oscillatoria sp. Morphotype 4 (Fig. 6d) The trichome is straight and long, with a biovolume of 822 $\pm$ 69 μm^3 for 50 μm. Cells are always shorter (1.4–5.0 μm) than wide (3.6–6.6 μm) with a ratio length/width of 0.63. The trichome counts approximately 19 $\pm$ 1.9 cells for 50 μm. The apex of the trichome does not exhibit clear differentiation from its base. The color of the trichome is bright blue-green, relatively homogeneous among cells. Pores, granules, and separation disks are not observed. Cells are not always easily distinguishable.

Remarks: Morphotype 4 was the most common *Oscillatoria* morphotype and was found in eleven samples from the four different locations. Mph 4 is distinguished from the other morphotypes by the high ratio of length/width and the color of the cells. This morphotype has the smallest biovolume at the filament level (50 μm).

Oscillatoria sp. Morphotype 5 (Fig. 6e) Trichome is short and straight or slightly curved, with a biovolume of 961 $\pm$ 40 μm^3 for 50 μm. Cells are shorter (1.5–4.9 μm) than wide (4.5–5.7 μm) with a ratio length/width of 0.57. Separation disks are observed but not always present. Sometimes pores are present in the chromoplasm or localized at the septa. Apical cells are not differentiated. Cells sometimes constricted at the cross-walls. Cells are yellowish-green to brownish.

Remarks: Mph 5 was systematically shorter than other trichomes. The morphotype was present in four samples, from Priestley and Nansen locations.

Oscillatoria sp. Morphotype 6 (Fig. 6f) The trichome is long, waved, without sheath and not constricted at the cross-walls. Separation disks are always observed, and cells have a green or brightly green color. Apical cells are usually conical and capitate. Cells are shorter (1.8–4.2 μm) than wide (4.7–5.9 μm) with a ratio length/width of 0.68. The biovolume of the trichome is 1018 $\pm$ 73 μm^3 for 50 μm.

Remarks: Mph 6 was present in only one sample from the Priestley location (biovolume $<$ 60 $\mu m^3\ g^{-1}$).

Crinalium glaciale var. helicoides (Fig. 7a) Single filament, trichome helically coiled, with a bright blue-green color. Separation disks are often observed. The biovolume of the trichome (50 μm) is high (7595 $\pm$ 873 μm^3). Cells are largely shorter (1.4–3.4 μm) than wide (11.3–15.8 μm), and well distinguishable. The species is characterized by a low ratio length/width (0.18 $\pm$ 0.0) and a high number of cells for each 50 μm-trichome (24 cells/50 μm).

Remarks: *Crinalium glaciale* has been described in the literature as a new species and previously reported among sediments of cryoconite holes on glaciers in Southern Victoria Land, Antarctica, by Broady and Kibblewhite (1991). Except for one occurrence of the species in soil found by Broady (2005), the taxa seems to be restricted to the particular habitats of cryoconite holes (Porazinska and others, 2004; Mueller and others, 2001; Mueller and Pollard, 2004). In our study, *Crinalium glaciale* var. *helicoides* was observed in three samples from Hells Gate and Tarn Flat locations (biovolume comprised between 3 and 63 $\mu m^3\ g^{-1}$).

Gloeocapsopsis sp. Morphotype 1 (Fig. 7b) The colonies form irregular, agglomerated, packet-like. Sheaths are sharply delimited, colorless, or slightly gold-yellow. Cells are spherical to irregular-spherical or semiglobose, most of the time with a brightly green color and more rarely greyish color, 3.1–6.9 μm in diameter (cellular biovolume of 58 $\pm$ 4 μm^3). The colonies can comprise a minimum of 4 cells, up to hundreds (difficult to distinguish). The cell division is irregular.

Remarks: Based on the classical literature, the taxon resembles the species *Gloeocapsopsis aurea* described by Mataloni and Komárek (2004) and Zidarova (2008) and seems to be a typical Antarctic species. However, in both previous papers, *Gloeocapsopsis aurea* was observed in the maritime region. The species *Gloeocapsopsis aurea* was also reported in microbial mats (Valdespino-Castillo, 2018) and in seepage habitats in Antarctica (Komárek and Komárek, 2010), and has been classified as 'probably endemic' by Komárek and Komárek (2010), as the species has not been found outside of Antarctica. In our study, *Gloeocapsopsis* sp. was exclusively observed in four samples from the Nansen location.

Gloeocapsopsis sp. Morphotype 2 (Fig. 7c) The *Gloeocapsopsis* sp. Morphotype 2 shares the same characteristics as Mph 1 except for the color of the sheath. In Mph 2, the sheaths are rusty yellow-brown to dark orange. The Mph 2 of *Gloeocapsopsis* sp. is always present together with Mph 1 and was observed in two samples from the Nansen location.

Nodularia sp. (Fig. 7d) Filaments are more or less straight or curved, relatively singular without forming mass populations. Trichomes are constricted at cross-walls. The heterocysts are present and spaced more or less regularly from each other, being larger than vegetative cells. Cells are light green to yellow-green. Vegetative cells are shorter (2.5–3.8 μm) than wide (6.4–7.7 μm) with a ratio length/width of 0.44. A colony of 50 μm counts approximately 16 vegetative cells and the biovolume of the colony is 1277 $\pm$ 59 μm^3.

Remarks: The genus *Nodularia* was previously reported in Antarctica in various regions, such as in meltwater ponds of the McMurdo Sound region (Jungblut, 2005; Jackson and others, 2021; Lizieri and others, 2022), and in aquatic habitats in the James Ross Island (Komárek and others, 2015). The species *Nodularia harveyana* was also reported in cryoconite holes in Antarctica by Wharton and others (1981). The consistent characters observed

https://doi.org/10.1017/jog.2025.12 Published online by Cambridge University Press

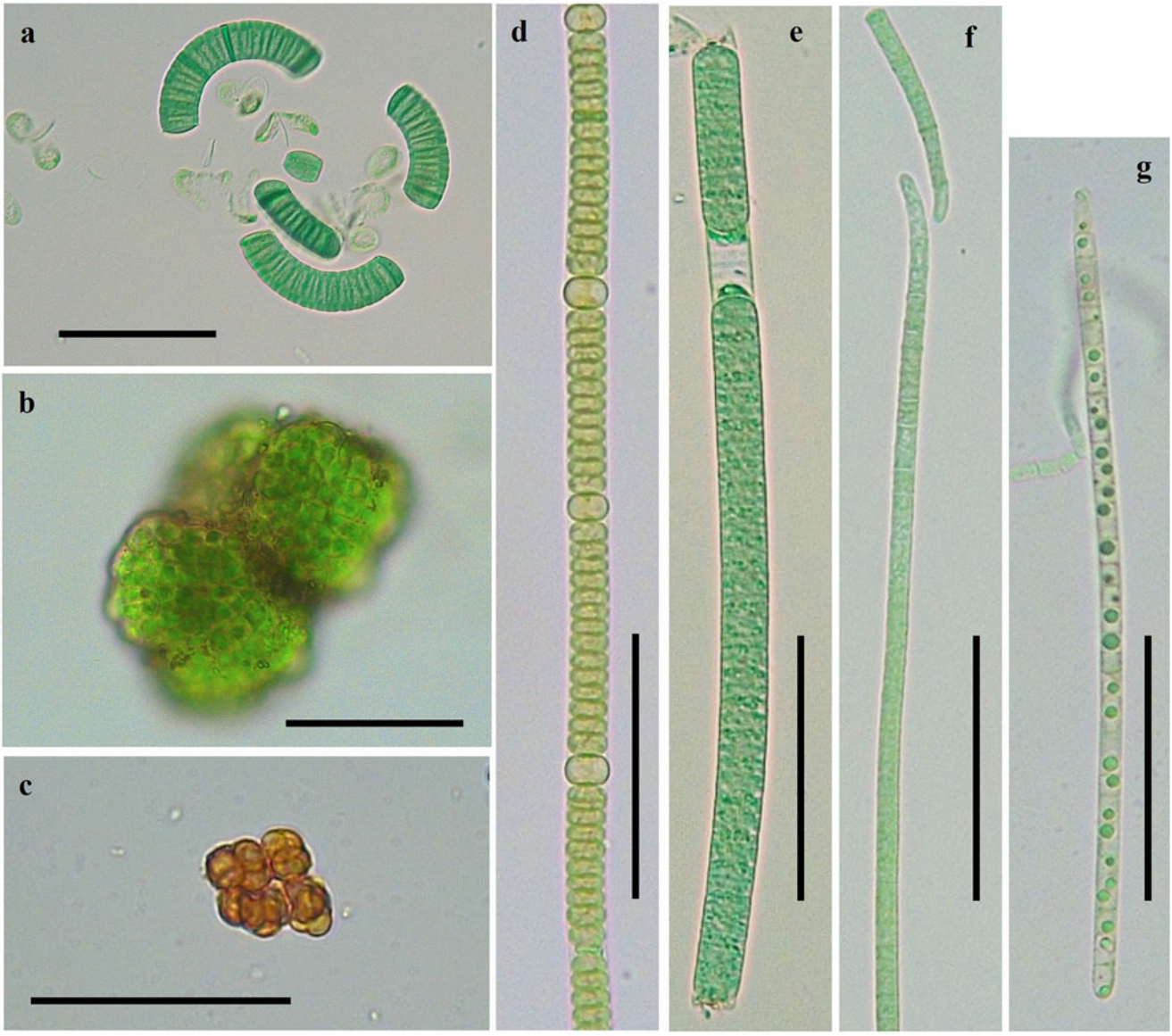

Figure 7. Species and morphotypes in cryoconite holes in Northern Victoria Land belonging to the Cyanophyceae. (a) *Crinalium glaciale* var. *helicoides* (Gomontiellales) (b–c) Species and morphospecies belonging to the Chroococcidiopsidales order: (b) *Gloeocapsopsis* sp. (Mph 1); (c) *Gloeocapsopsis* sp. (Mph 2). (d) *Nodularia* sp. (Nostocales) (e–g) Species and morphotypes belonging to the Oscillatoriales order: (e) Lyngbya sp.; (f) *Phormidium* sp. (Mph 1); (g) *Phormidium* sp. (Mph 2). Black scales represent 50 μm.

allowed assignment to *Nodularia* cf. *quadrata*. The taxon was present in only one sample from the Hells Gate location (biovolume of 398 $\mu m^3\ g^{-1}$).

Lyngbya sp. (Fig. 7e) Filamentous trichome, solitary, straight. The sheath is almost always visible, firm, thin, and colorless. Cells are green, sometimes yellowish, shorter (3.1–5.2 μm) than wide (7.6–8.6 μm) with a ratio length/width of 0.51, not constricted at the cross-walls, without pores or granules. The biovolume of the trichome is 2673 ± 380 μm^3 for 50 μm. End cells are often attenuated.

Remarks: The taxon was observed in only one sample from the Tarn Flat location (biovolume of 8.3 $\mu m^3\ g^{-1}$), together with *Phormidium* and *Oscillatoria* morphotypes.

Phormidium sp. Morphotype 1 (Fig. 7f) Filamentous trichomes, straight and long, not constricted at the cross-walls, without sheath. Cells are quadratic or longer than wide (length 2.1–7.3 μm and width 1.6–5.2 μm) with a ratio length/width of 1.0. Cells are green to blue-green, without granules. Apical cells are slightly pointed and curved. The biovolume of the trichome is relatively small (938 ± 165 μm^3 for 50 μm).

Remarks: The *Phormidium* Mph 1 was among the most observed taxon and was present in nine samples from the four locations. The distinction between the *Oscillatoria* morphotypes was based on the length/width ratio.

Phormidium sp. Morphotype 2 (Fig. 7g) Filamentous trichomes, relatively short and straight, not constricted at the cross-walls, without visible sheath. Cells are quadratic or longer (3.0–5.9 μm) than wide (3.1–5.0 μm) with a ratio length/width of 1.1. Cells are colorless to green or yellowish, characterized by the presence of large blue-green granules in the centroplasm. The

https://doi.org/10.1017/jog.2025.12 Published online by Cambridge University Press

biovolume of the trichome is small (735 ± 99 μm^3 for 50 μm). Apical cells are slightly constricted and conical.

Remarks: The *Phormidium* Mph 2 was observed in eight samples from all locations except Priestley.

Anagnostidinema sp. (Fig. 8a) Filamentous trichome, thin and solitary, cylindrical, without sheath. Cells are not constricted at the cross-walls, elongated, always longer (2.2–2.7 μm) than wide (1.0–1.5 μm) with a ratio length/width of 2.2. Cell color is usually olive green to greyish and cells are not always easily distinguishable from each other. Apical cells are usually conical, hooked, or bent. The biovolume of the trichome is one of the smallest, with 63 ± 3 μm^3 for 50 μm.

Remarks: Morphological characteristics of the taxon could allow assignment to the genus *Geitlerinema*, which has been documented many times (Komárek, 1999; Taton and others, 2006; Lizieri and others, 2022), indicating that the genus is widely distributed across Antarctica. However, according to Johansen (2017), the taxon observed in our samples should present more characteristics of *Anagnostidinema,* especially because of the absence of capitate apical cells. Nevertheless, these two taxa are morphologically highly similar, and the main difference must be observed in the secondary structure of conserved domains of the 16S–23S ITS region by molecular analyses. In our study, *Anagnostidinema* sp. was observed in only two samples from the Hells Gate location (biovolume comprised between 10 and 85 μm^3 g^{-1}).

Pseudanabaena sp. (Fig. 8b) Trichomes solitary, usually straight or a little waved, consisting of few to several cells, with broad constrictions at cross-walls. Cells are cylindrical, usually longer (1.6–4.3 μm) than wide (1.0–2.4 μm) with a ratio length/width of 1.6. Cells are blue-green or greyish, apical cells are not differentiated. The cellular biovolume is small (5.2 ± 0.5 μm^3).

Remarks: Morphological features of this taxon were consistent with the species *Pseudanabaena galeata*. The genus *Pseudanabaena* was often observed in Antarctic regions and has been shown to be important for the formation of the microbial mat matrix structure as found in ponds in the McMurdo Dry Valleys (Jungblut and Vincent, 2017; Lizieri and others, 2022). In our study, *Pseudanabaena* sp. was observed in 21 samples from the four locations.

Komphovoron sp. (Fig. 8c) Trichome is a solitary filament, often straight or slightly flexuous. The filament is short and composed of several cells. The cells are spherical to barrel-shaped and relatively small. The end cells are mostly rounded. Necridic cells, akinetes, aerotopes and heterocysts were not observed. The cells are slightly shorter (2.7–4.1 μm) than wide (3.2–4.6 μm) with a ratio length/width of 0.85. Cells are bright blue-green to green. The biovolume of the trichome is 457 ± 20 μm^3 for 50 μm.

Remarks: The genus *Komphovoron* was recently observed among benthic cyanobacterial assemblages in meltwater ponds in the McMurdo Sound region in Antarctica (Lizieri and others, 2022). However, to date, no studies have reported the presence of the taxon in cryoconite holes. In our study, the genus *Komphovoron* sp. was only present in one sample from the Tarn Flat location (at low occurrence, biovolume < 1 μm^3 g^{-1}).

Nostoc cf. microscopicum (Fig. 8d) Filaments always form a dense, gelatinous mat of constricted cells. The mucilage of the colony is firm and varies from colorless to brownish. The vegetative cells are highly spherical (4.2–4.8 μm in diameter), with a uniform shape and size along trichome, bright blue-green or olive-green. Heterocysts are larger than vegetative cells, also spherical (approximately 7 μm in diameter). Colonies are large, often several tens of micrometers.

Remarks: The taxon was observed punctually (i.e. in one exemplary as a colony) in three samples from Nansen and Tarn Flat locations. The genus has been documented in a wide range of Antarctic habitats (Broady, 2005; Komárek and Elster, 2008; Fernández-Carazo and others, 2012; Lizieri and others, 2022).

Stigonema minutum (Fig. 8, e1–e2) The filament (18–28 μm width) is composed of individual cells arranged in one row in the sheath. The cells are spherical or elliptic, 5.0–10.4 μm long and 11.4–13.5 μm wide, with a ratio length/width of 0.65. Each cell has an individual sheath within the common sheath. No heterocyst was observed.

Remarks: The morphological features of the taxon were consistent with *Stigonema minutum* described by Ohtani and Kanda (1987). Taxa belonging to the *Stigonema* genus have been previously reported in Antarctica, in moss or soil samples (Ohtani and Kanda, 1987; Fernández-Carazo and others, 2012; Das and Singh, 2021; Yakushev, 2022) but to date, the taxon is not reported in cryoconite holes. In our study, one specimen of *Stigonema minutum* was observed in only one sample from the Nansen location (at low occurrence, biovolume < 1 μm^3 g^{-1}).

Pleurocapsa sp. Morphotype 1 (Fig. 8f) Colonies form irregular branching aggregates of light-green cells. Sheath is most of the time colorless and thin. Cells are spherical or ovoid with sides appressed by neighboring cells. The diameter of single cells is 3.0–8.3 μm. Cells are united laterally by the confluence of thin gelatinous sheaths.

Remarks: Morphological characteristics of this genus are consistent with the species *Pleurocapsa minor* described by Shalygin (2019). The genus *Pleurocapsa* has been documented in Antarctica, mainly in coastal, maritime Antarctica (Komárek, 2014; Velichko and others, 2021). To date, it seems that this genus has not been reported in cryoconite substrate. *Pleurocapsa* sp. was observed in only one sample of the Tarn Flat location (biovolume < 5 μm^3 g^{-1}).

Pleurocapsa sp. Morphotype 2 (Fig. 8g) The *Pleurocapsa* sp. Morphotype 2 shares the same characteristics as Mph 1 except for the color of the sheath. In Mph 2, the sheaths are rusty yellow-brown to dark orange.

Chroococcus sp. (Fig. 8h) Colonies are generally in groups of two cells. Grouped cells remain hemispherical, mucilaginous envelopes not always visible. Cells widely oval, blue-green to yellowish with homogeneous content. Cell diameter is relatively small, 3.4–6.0 μm.

Remarks: The genus *Chroococcus* sp. was observed in three samples from the Hells Gate and Nansen locations.

2. Green algae

Klebsormidium flaccidum (Fig. 9a) Filament is long, not constricted. Cells are cylindrical, longer (3.0–12.4 μm) than wide (6.8–9.7 μm). The chloroplast covers approximately 2/3 of the cell

https://doi.org/10.1017/jog.2025.12 Published online by Cambridge University Press

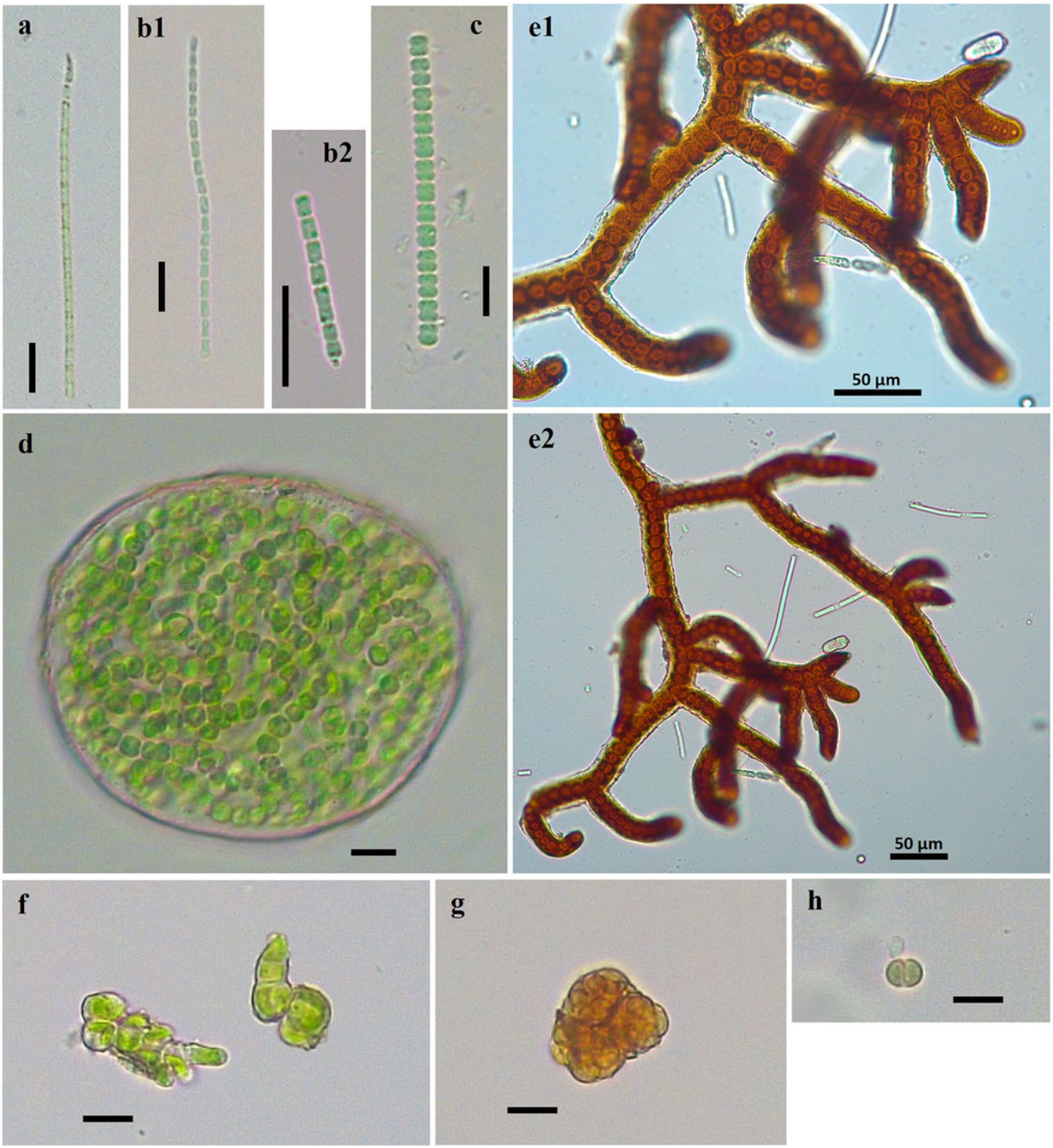

Figure 8. Taxa and morphotypes in cryoconite holes in Northern Victoria Land belonging to the Cyanophyceae. (a) *Anagnostidinema* sp. (Coleofasciculales); (b) *Pseudanabaena* sp. (Pseudanabaenales); (c) *Komphovoron* sp. (Gomontiellales); (d) *Nostoc* cf. *microscopicum* (Nostocales); (e) *Stigonema minutum* (Nostocales); (f–h) morphotypes belonging to the Chroococales order: (f) *Pleurocapsa* sp. (Mph 1); (g) *Pleurocapsa* sp. (Mph 2); (h) *Chroococcus* sp. Black scales represent 10 µm except for e1–e2.

inner surface, with smooth margins. Filaments are smooth and relatively flexuous. Cells are bright green.

Remarks: The morphological features of the taxon are consistent with the species *Klebsormidium flaccidum* which has been reported in several habitats in Antarctica (Borchhardt, 2017; Rippin and others, 2019), other glacial environments such as alpine biological soil crusts (Mikhailyuk and others, 2015) and cryoconite holes in the Arctic (Kaštovská and others, 2005; Stibal and others, 2006). In our study, the taxon was present in only one sample from the Hells Gate location (biovolume of 102 $\mu m^3\ g^{-1}$).

Chlamydomonadales—motile stage (Fig. 9b) During the motile-vegetative (green) stage, Chlamydomonadales cells are flagellated, and the chloroplast is basal and bright green. The cell

https://doi.org/10.1017/jog.2025.12 Published online by Cambridge University Press

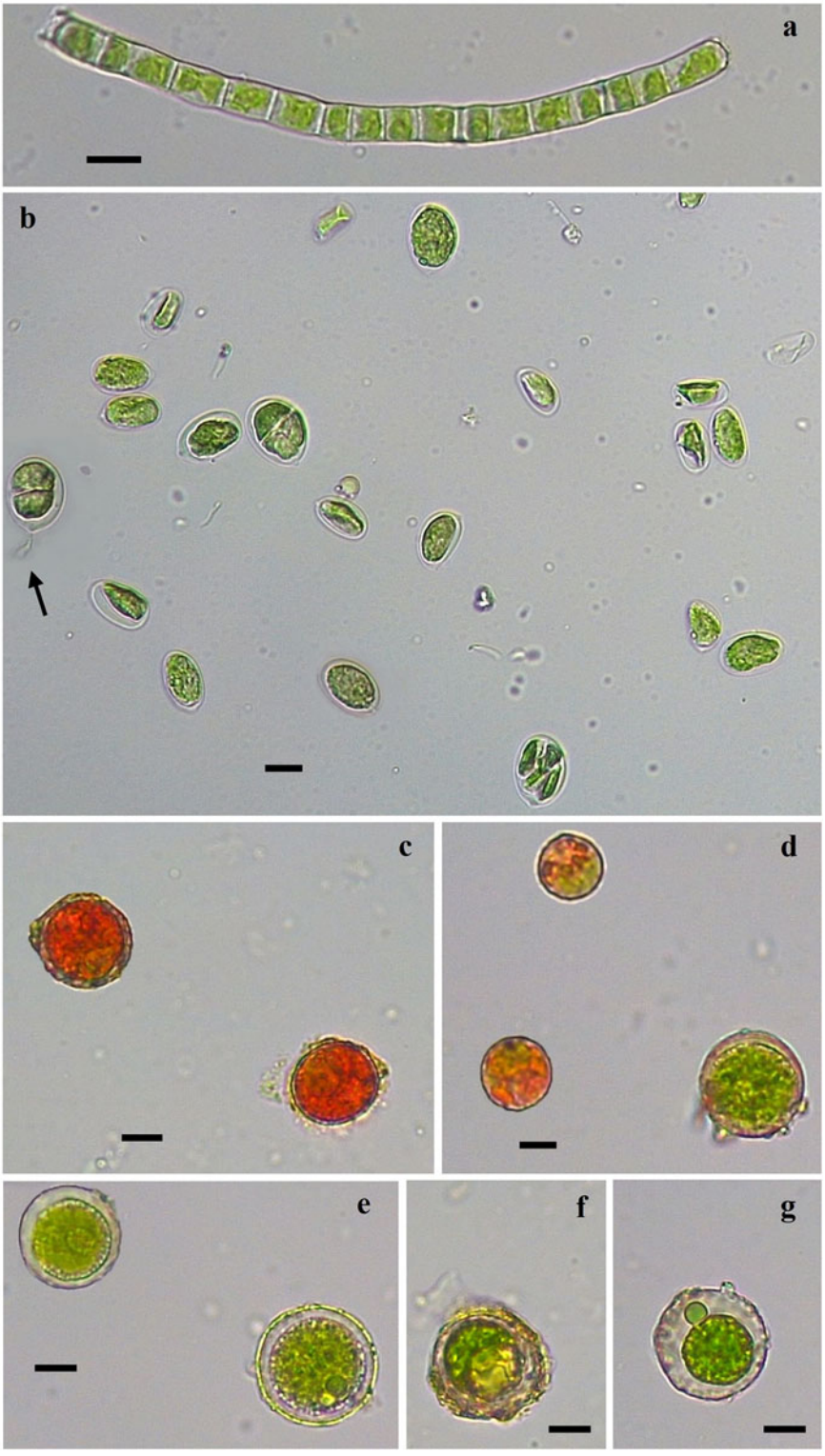

Figure 9. Microalgae species in cryoconite holes in Northern Victoria Land belonging to the Klebsormidiophyceae and Chlorophyceae. (a) *Klebsormidium* flaccidum; (b) Chlamydomonadales flagellated phase; (c–g) diverse cyst-like stage of *Sanguina* sp. (c) red cyst phase; (d) green–red cyst phase; (e–g) green cyst phase. Black scales represent 10 μm.

wall is firm and well-distinguishable. Sometimes, mitotic division is observed. The size of the cells during the flagellate phase is 6.7–28.6 μm long and 4.9–28.6 μm wide. The cellular biovolume is relatively high (1456 ± 337 μm^3). Cells are highly motile.

Sanguina sp. (Fig. 9c–g) The cyst-like stage varies in size and color, from bright red (Fig. 5c) and green-orange (Fig. 5d) to green (Fig. 5e–g). Mature red cysts are highly pigmented, with a condensed chloroplast and a firm, thick cell wall. Cysts diameters are 7.4–35.8 μm with a cellular biovolume 2147 ± 238 μm^3. Transient, young, green-orange cysts vary from visible green parts of the chloroplast to totally red-orange pigmentation. The diameters of the green-orange cysts are similar to the red stage, but more variable (15.9 ± 1.3 μm), while the cellular biovolume is slightly

https://doi.org/10.1017/jog.2025.12 Published online by Cambridge University Press

higher (2825 ± 739 μm^3). The green-cyst stage has irregular, non-lamellate chloroplast, sometimes concentrated in the central part of the cyst. The cell wall is firm, most of the time colorless, sometimes irregular, and covered with small particles. The green-cysts present the highest diameter (19.4 ± 1.2 μm) and the highest biovolume (5121 ± 846 μm^3).

Remarks: The cyst-like stage of the *Sanguina* sp. belongs to the blood snow algae, often found in Antarctic habitats (Luo, 2020; Procházková and others, 2021). Especially, this taxon is mainly found in melting snow (Procházková and others, 2019), in the ablation zone of glaciers (Di Mauro, 2020) and the accumulation zones, and in proglacial environments (Di Mauro, 2024). Reads of *Sanguina* sp. were detected by using 18S rDNA marker in the cryoconite of the Forni Glacier (Italy) (Zawierucha, 2022). As it is not possible to assign the flagellated stage to the blood snow algae without molecular description, we distinguished between the motile stage of Chlamydomonadales and the cyst-like stage of *Sanguina* sp. In our samples, the green and green-orange cyst-like stages of *Sanguina* sp. were observed in 19 and 12 samples, respectively. The red cyst stage and the motile flagellated stage were observed in nine samples.

3. Diatoms

Achnanthidium sp. (Fig. 10, a1–a2) Cells are relatively small, with cellular dimensions of 16.2–25.4 μm long and 3.6–5.7 μm wide, with a ratio length/width of 4.18. The valve is elliptic with ends obtusely to rounded. The raphe is filiform, straight, with a central area not highly developed. The number of striae is 15/10 μm. The cellular biovolume is of 537 ± 215 μm^3.

Remarks: Diverse species of *Achnanthidium* have been found in cryoconite holes and glacial ponds around the world (Yallop and Anesio, 2010; Pinseel and others, 2015; Kaczmarek and others, 2016), and in streams and small water bodies in the King George Island region in Antarctica (Zębek and others, 2021). In our study, *Achnanthidium* sp. was observed in nine samples, from Nansen, Priestley (low occurrence, i.e. biomass < 0.1 μg g^{-1}), and Hells Gate (high occurrence, i.e. biovolume > 500 μm^3 g^{-1}).

Luticola gaussii (Fig. 10, b1–b2) The valve is elliptic-lanceolate, with ends broadly rounded. The margins are symmetrical, convex, and rounded in central area and the apices are broadly rounded and capitate. An isolated pore is present in the central area, located halfway between valve center and valve margin. The central area is rectangular, bordered by shortened striae on both sides. Cell dimensions are 13.6–33.1 μm long and 7.7–11.1 μm wide, with a ratio length/width of 2.33. The number of striae is 18–20(22)/10 μm. The cellular biovolume of the species is 1251 ± 181 μm^3. The central area consists of a moderately wide fascia ranging to the margins.

Remarks: The morphological features of the taxon are consistent with the species *Luticola gaussii*. The taxon was observed in 17 samples from the four locations (biovolume comprised between 0.04 and 350 μm^3 g^{-1}). Species of the genus *Luticola* are typical for terrestrial ecosystems in the Antarctic Region (Kopalová and others, 2011; Van de Vijver and others, 2011) and have been described in detail by Kohler and others (2015).

Luticola muticopsis (Fig. 10, c1–c2) Cell dimensions are 10.0–18.0 μm long and 7.0–9.8 μm wide, with a ratio length/width of 1.77. The valve is elliptic with ends flat to broadly rounded. The number of striae is 17/10 μm. The cellular biovolume of the species is 736 ± 131 μm^3. The central area consists of a moderately wide fascia ranging to the margins.

Remarks: The characteristic features of the taxon were consistent with *Luticola muticopsis,* described in detail by Bishop (2020) and Kohler and others (2015). The taxon was distinguished from *Luticola gaussii* by cell length and striae number. The taxon was observed in 10 samples from Priestley, Nansen and Hells Gate locations (biovolume comprised between 0.04 and 542 μm^3 g^{-1}).

Cymbella sp. (Fig. 10, d1–d2) The valve is moderately dorsiventral, lanceolate-elliptic. The dorsal margin is more strongly convex than the ventral margin, which is slightly radiate throughout. The axial area is narrow, following the raphe, which is positioned about in the median line of the valve. Cell dimensions are 24.3–50.2 μm length and 7.3–13.9 μm wide, with a ratio length/width of 3.6. The number of striae is 10–11/10 μm and the number of stigma are 2. The cellular biovolume is 2106 μm^3.

Remarks: Other species belonging to the *Cymbella* genushave been previously reported in Antarctica. For example, *Cymbella* cf. *falaisensis* was observed in the sediment of Lake Hoare (Taylor Valley), in the McMurdo Dry Valleys region of Southern Victoria Land, Antarctica (Spaulding and others, 1997). The species *Cymbella proxima* has also been reported among the periphytic algae assemblages of microbial mats in streams and small water bodies in the vicinity of Ecology Glacier (King George Island, Antarctica) (Zębek and others, 2021). In our study, *Cymbella* sp. was counted in only one exemplary in one sample from the Hells Gate location.

Nitzschia angustata (Fig. 10e) The valve is linear, tapering to the obtusely wedge-shaped ends. Cell dimensions are 38.1–38.4 μm long and 3.4–3.5 μm wide, with a ratio length/width of 11.2. The number of striae is 15/10 μm. Fibulae are not distinguishable. The cellular biovolume is 1034 ± 12 μm^3.

Remarks: The morphological characteristics were consistent with the species *Nitzschia angustata* (synonym *Tryblionella angustata*). The taxon was observed in only one sample from Hells Gate location (at low occurrence, biovolume < 1 μm^3 g^{-1}).

Psammothidium rostrogermainii (Fig. 10, f1–f2) The valve is broadly elliptic-lanceolate with ends abruptly rostrate. Cell dimensions are 13.3–16.5 μm long and 7.4–9.0 μm wide, with a ratio length/width of 1.9. The number of striae is 12/10 μm but slightly variable. The cellular biovolume is 436 ± 13 μm^3.

Remarks: The morphological features of the taxon were consistent with the species *Psammothidium rostrogermainii,* described by (Van de Vijver and others, 2016). The taxon has been identified by the authors in the Antarctic Region, and was observed on several islands of the South Shetland Archipelago (Livingston Island, King George Island, Nelson Island, Dart Island, and Deception Island) and James Ross Island. It should be much more common in the Antarctic but usually identified as *P. germainii* (Van de Vijver and others, 2016). In our study, the taxon was observed in 7 samples from the four locations (biovolume comprised between 0.2 and 382 μm^3 g^{-1}).

Craticula cf. antarctica (Fig. 10, g1–g3) The valve is broadly lanceolate to rhombic lanceolate with ends protracted, subrostrate. Cell dimensions are 17.3–18.5 μm long and 3.4–5.3 μm wide, with a ratio length/width of 3.9. Striae almost parallel to very slightly radiate in the valve center, becoming slightly convergent. The number

https://doi.org/10.1017/jog.2025.12 Published online by Cambridge University Press

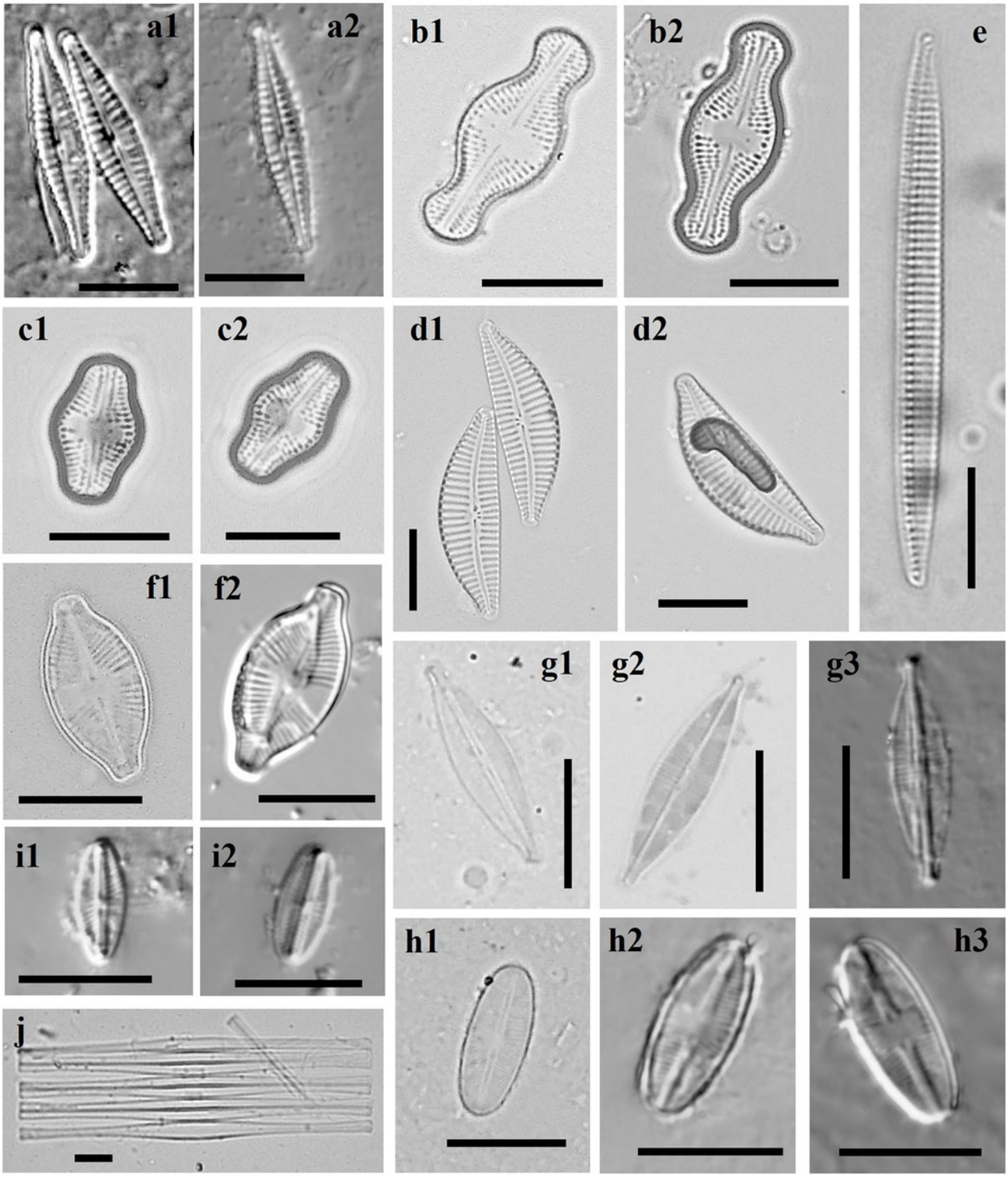

Figure 10. Microalgae species in cryoconite holes in Northern Victoria land belonging to the Bacillariophyceae. (a1–a2) *Achnanthidium* sp.; (b1–b2) *Luticola gaussii*; (c1–c2) *Luticola muticopsis*; (d1–d2) *Cymbella* sp.; (e) *Nitzschia angustata*; (f1–f2) *Psammothidium rostrogermainii*; (g1–g3) *Craticula* cf. *antarctica*; (h1–h3) *Psammothidium* cf. *helveticum*; (i1–i2) *Mayamaea* sp.; (j) *Fragilaria* sp. Black scales represent 10 μm.

https://doi.org/10.1017/jog.2025.12 Published online by Cambridge University Press

of striae is 28–30/10 μm, relatively difficult to resolve. The central area is not visible and the raphe branches are straight and filiform. The cellular biovolume is 327 ± 14 μm^3.

Remarks: The morphological characteristics resemble those of *Craticula antarctica* described by Van de Vijver (2010). The morphological features could also correspond to *Craticula simplex* described by Levkov (2016) and to *Craticula autralis* described by Van de Vijver and others (2015) from one sample, taken from the epilithon of a shallow coastal lake on Ulu Peninsula (James Ross Island, Antarctica). The taxon was observed in two samples, in Hells Gate (biovolume of 44 $\mu m^3\ g^{-1}$) and Nansen locations (biovolume of 28 $\mu m^3\ g^{-1}$).

Psammothidium cf. helveticum (Fig. 10, h1–h3) The valve is elliptic to linear-elliptic, with ends broadly rounded. Cell dimensions are 12.8–14 μm length and 5.0–5.9 μm width, with a ratio length/width of 2.4. The number of striae is 24–28 in 10 μm, difficult to resolve in the smallest specimens. The central area forms a fascia that almost reaches the margins. The cellular biovolume is 195 ± 4 μm^3.

Remarks: Taxon similar to *P.* cf. *helveticum* was previously found in soil under vegetation cover in the Antarctic Region by Zidarova and others (2016a). In our samples, *P.* cf. *helveticum* was observed in only one sample from Hells Gate location (at low occurrence, biovolume of 4.9 $\mu m^3\ g^{-1}$).

Mayamaea sp. (Fig. 10, i1–i2) The valve is rhombic-lanceolate to rhombic-elliptic with rounded to obtusely-rounded apices. Cell dimensions are 9.1–10.2 μm long and 3.5–4.2 μm wide, with a ratio length/width of 2.52. The central area is small and the raphe is straight. Striae number is difficult to resolve due to the small size of the cells, approximately 20 in 10 μm. The raphe is filiform, with distinct central pores. Cell biovolume is 80 ± 3 μm^3.

Remarks: The morphological characteristics of the taxon and the dimensions of the cells were consistent with the *Mayamaea* genus, in particular with the species *Mayamaea* cf. *atomus* described by Zidarova and others (2016a). The general features could also be consistent with the genus *Eolimna*, however, the cell dimensions are too small and should better correspond to *Mayamaea* (Kopalová and others, 2009). The genus *Mayamaea* has already been reported in Antarctica, in a lake on Ulu Peninsula (James Ross Island), and small crack of a coastal rock on Deception Island (South Shetland Islands) (Zidarova and others, 2016b). The visible morphological features of the taxon do not allow to determine more precisely the taxonomic level. In our study, *Mayamaea* sp. was observed in only one sample from the Priestley location (biovolume of 7 $\mu m^3\ g^{-1}$).

Fragilaria sp. (Fig. 10j) The valve is narrow, linear to lanceolate. The cell dimension is 94.1 ± 1.8 μm length and 4.0 ± 0.2 μm width, with a ratio length/width of 23.4.

Remarks: The cell dimensions could correspond to *Fragilaria tenera, F. perdelicatissima* and *F. nanana*, however, the absence of visible determination criteria and the scarce observation of individuals make the identification of the species very difficult. Nonetheless, *Fragilaria* species have been observed in meltwater lakes in the Amery Oasis, East Antarctica (Cremer and others, 2004), but also in Marian Cove of King George Island, Antarctica (Jeon, 2021) and in cryoconite holes in the Arctic (Greenland and Svalbard) (Yallop and Anesio, 2010). As for the other unique specimens found in this study, other observations are needed to confirm the presence of *Fragilaria* sp. in the cryoconite holes of the Northern Victoria Land region.

4. Discussion

4.1. Distribution of Cyanobacteria and microalgae

This study describes the diversity and composition of Cyanobacteria and microalgae assemblages in cryoconite holes from the Northern Victoria Land, East Antarctica. We observed that cryoconite holes were mostly dominated by Chlorophytes, followed by Cyanobacteria. Although these two groups were found in almost equal proportion (in terms of relative biomass in all locations), these findings were rather unexpected. Indeed, Cyanobacteria are traditionally dominant in cryoconite holes and are considered 'engineers' of these ecosystems, due to their role in the formation of granular cryoconite (Takeuchi and others, 2001; Hodson, 2008; Cook and others, 2016). However, similar results with a dominance of algae over Cyanobacteria have also been observed by Buda (2020) in the cryoconite holes from the Ecology Glacier (King George Island, located between 61°54′—62°16′S and 57°35′–59°02′W, West Antarctica). The authors suggested that the dominance of algae over Cyanobacteria should be caused by the fact that tidewater glaciers located close to the sea may receive more aqueous nutrients that favor algae. In contrast, inland ice sheets and small valley glaciers may receive more inputs of dust or englacial outcropping minerals, favoring Cyanobacteria that bind particles and form granules. In our study, this assumption is consolidated by the elevated electrical conductivities, which likely indicate a strong proximity with the ocean, and therefore possible exchanges of marine nutrients, especially in Hells Gate samples which are the closest to the sea. Our results confirm that microalgae, especially Chlorophytes, are a crucial component of the cryoconite ecosystems.

While the algal biovolume and diversity did not differ within the glacial locations, we observed significant differences in the total biovolume, the Shannon diversity, and the richness of genera among the four locations. At the opposite, the community composition (at the genus level) did not significantly vary among the four locations. In a recent molecular study, Segawa (2017) showed that, within a glacial environment, some species of Cyanobacteria presented a ubiquitous distribution due to low sensitivity to environmental conditions, while the distribution of other species was more specific, mainly determined by the regional characteristics in glaciers, due to high sensitivity to different environmental conditions. In our study, we can assume that both environmental conditions and geographical distance among the four glacial locations were not enough to observe a significant difference in taxa composition. However, regarding the morphotypes of *Oscillatoria* species, of the 6 morphotypes distinguished, one (Mph 4) was present in all glacial locations, and another (Mph 6) was present in a unique location (Priestley). These results could indicate a higher sensitivity of Mph 6 to specific environmental conditions and a lower sensitivity of Mph 4, which showed a ubiquitous occurrence among the locations.

The Shannon diversity values calculated at the genus level ranged between 0.04 and 1.7, and the richness of genera ranged between 2 and 11 taxa, with the highest values of diversity and richness observed in the Hells Gate and Tarn Flat samples. Studies that compare photoautotroph biomass and diversity among cryoconite holes from different locations are quite rare; to date, Buda

https://doi.org/10.1017/jog.2025.12 Published online by Cambridge University Press

(2020) found no differences in the total biomass of photoautotrophs among three elevational patches of an altitudinal gradient of Ecology Glacier. In our study, the Hells Gate location was characterized by the highest biovolume and high diversity and richness. In addition, this location was also characterized by a higher proportion of diatoms (20.4%) than in the three other locations (19.2% in Priestley, 3% in Tarn Flat, and <1% in Nansen). Previous studies have hypothesized that cryoconite holes are predominantly seeded by aeolian transport from surrounding aquatic environments (Christner and others, 2003; Budgeon and others, 2012). Moreover, diatoms are first-colonizers and have a high range of ecological tolerances, including freeze-thaw conditions (Yallop and Anesio, 2010). For example, in a previous study in the Taylor Valley, Antarctica, Stanish and others (2013) observed a higher diatom richness in the cryoconite holes situated closest to the Ross Sea.

The diatom species observed in the cryoconite holes from the Hells Gate locations seemed not particularly restricted to marine environments, as the taxa were already observed in other habitats such as cryoconite holes, ponds, terrestrial systems, or microbial mats. However, due to the higher proximity of the Hells Gate samples to the sea, we can argue that the high biovolume, diversity, richness, and diatom proportion in these samples may be attributed to the inputs of marine nutrients. Indeed, eolian transportation of sea salts may occur, which deposits into the cryoconite hole and acts as an important source of solute (Mueller and Pollard, 2004; Bagshaw and others, 2013). The proximity of colonies of penguins and seals from Hells Gate samples could also act as a means of diffusion of nutrients. In the Tarn Flat location, the proximity of terrestrial habitats and moraines close to the sampling sites may explain the relatively high diversity and richness, although only two samples were available for this location and thus results must be interpreted with caution. The characteristics of cryoconite, including its forms and geochemistry, can also influence their effect on glacier albedo and act as important factors in determining the algal community (Rozwalak, 2022). The cryoconite sediment from the four glacial locations of this study showed a slight diversity in terms of size, form, and colors. The observed differences in algal biovolume and diversity could thus also be explained by differences in cryoconite structure, although further studies are needed to evaluate the specific effect of cryoconite characteristics on the photoautotroph community.

The number of taxa and the diversity of Cyanobacteria and microalgae in the cryoconites of the Northern Victoria Land appears consistent with previous studies in Antarctica. For example, in 23 melted cryoconite holes on Ecology Glacier (King George Island, Antarctica, situated at a distance of about 4500 km from the Northern Victoria Land), Buda (2020) observed 17 species of algae and Cyanobacteria with a biomass of 0.79 to 5.37 μg cm^{-3}, and each cryoconite hole was reported 4 to 10 species. However, photoautotrophic diversity and richness based on microscopic analysis in cryoconite holes are not well known. Most of the studies use molecular analysis to estimate the alpha diversity, pooling together bacteria and Cyanobacteria. For example, based on alpha diversity indices calculated on amplicon sequence variants, Millar and others (2021) found Shannon values in Antarctic cryoconite from 3.8 and 8 for prokaryotes (based on 16S rRNA gene analysis) and from 2.1 to 6.4 for eukaryotes (based on 18S rRNA gene analysis), which makes the results difficult to compare. Although diversity data from these studies show relatively similar ranges of values, the number of species or taxa detected in the samples depends largely on the methodology. This highlights the difficulty in comparing these results and the need to further use standard microscopy counting methods in addition to molecular analyses.

If the photoautotroph diversity of Antarctic cryoconite holes is still poorly known, values can be compared with other types of habitats in Antarctica, where more data is available. For example, a Shannon index of 1.1 was found for the periphytic assemblages in the microbial mats in the region of Arctowski Polish Antarctic Station at King George Island (West Antarctica) (Zębek and others, 2021). Microbial mats are often composed of organic and mineral particles that form a structural system of mats in streams and small water bodies located in the vicinity of the glacier. In highly diverse environments, i.e. underwater marine rocky substratum in Fildes Bay (King George Island, West Antarctic Peninsula), the species richness of primary producers ranged between 2 and 7 species, and the Shannon diversity between 0.2 and 1.2 (Valdivia and others, 2020). However, higher algal diversity (between 0.76 and 3.12, with an average of 2.30) was observed in soil samples from Cierva Point (Antarctic Peninsula) (Mataloni and others, 2000). Similarly, a Shannon diversity between 1.2 and 4 was observed in soil samples from King George Island, Maritime Antarctica (Rybalka, 2023). These findings indicate that (1) data on photoautotroph diversity in Antarctic habitats are incredibly scarce, and (2) the values of photoautotroph diversity observed in cryoconite holes in the Northern Victoria Land are equal to higher than those observed in other habitats such as marine rocky substrates, microbial mats, and snow surfaces but lower than those measured in soils. In addition, if the methodology used in this study has shown effectiveness in extracting algal cells from cryoconite, a slight underestimation of photoautotroph biovolume and diversity due to cells remaining attached to particles cannot be excluded. This suggests that algal diversity in cryoconites could be even higher, and that further in-depth studies are needed to more accurately understand photoautotrophic communities in cryoconite holes.

4.2. Description of the taxa

In total, 36 morphotypes from 24 taxonomic genera belonging to Cyanobacteria, Chlorophytes, Charophytes, and diatoms were described. Taxa belonging to 14 diverse taxonomic orders were observed, revealing a high taxonomic diversity in the samples. Among the identified taxa, some of them are relatively ubiquitous and found in a large variety of environments and climates, such as the *Lyngbya, Oscillatoria, Phormidium*, and *Pseudanabaena* genera. Interestingly, the N_2-fixing *Nostoc* cf. *microscopicum* identified in this study has been documented in a wide range of Antarctic habitats (Broady, 2005; Komárek and Elster, 2008; Fernández-Carazo and others, 2012; Lizieri and others, 2022).

It has been demonstrated that the metabolic activities of *Nostoc* strains in Antarctica, such as N_2-fixation, nitrate uptake, nitrate-reduction, ammonium uptake, and photosynthesis, were unaffected at low temperatures (5°C) and the temperature optima for N_2-fixation was nearly 10°C lower than their respective reference strains of tropical origin (Pandey, 2004). These findings indicate a high level of low-temperature adaptation of the *Nostoc* species in Antarctica. In addition, a recent molecular study demonstrated that *Nostoc* OTU also presented a global distribution, indicating that the taxon migrates among glacial regions (Antarctic, Arctic, and Asia) (Segawa, 2017).

Some taxa of photoautotrophs are specially adapted to life within the cryoconite holes, while others are opportunistic (Mueller and others, 2001; Yallop and Anesio, 2010; Cameron and others, 2012). In the cryoconite from the Northern Victoria

https://doi.org/10.1017/jog.2025.12 Published online by Cambridge University Press

Land, we observed the taxon *Crinalium glaciale*, which seems to be restricted to the particular habitats of cryoconite holes (Porazinska and others, 2004; Mueller and others, 2001; Mueller and Pollard, 2004). Instead, the taxon *Nodularia* sp. has been reported in cryoconite holes in Antarctica but also in other habitats such as meltwater ponds and aquatic habitats (Jungblut, 2005; Komárek and others, 2015; Jackson and others, 2021; Lizieri and others, 2022). Similarly, species of the genus *Luticola* have been shown to be typical for terrestrial ecosystems in the Antarctic Region (Kopalová and others, 2011; Van de Vijver and others, 2011). The presence of these two taxa in the sediment of cryoconite may thus be explained by the proximity of cryoconite holes with other types of habitats, the ability of species to colonize new environments, and the wide range of ecological tolerance of organisms.

Finally, several taxa observed in the cryoconite holes from the Northern Victoria Land have been previously documented in Antarctica but have not been reported to date in cryoconite. This is the case for *Gloeocapsopsis* sp., *Komphovoron* sp., *Stigonema* sp., and *Pleurocapsa* sp. Regarding the diatoms, several taxa found in this study were to date not described in cryoconite holes; for example, the genus *Mayamaea* has been reported in soil samples, lakes, and in small cracks of coastal rocks, and the genera *Luticola* is typical for terrestrial ecosystems. However, diatoms are first colonizers (after bacteria) of newly exposed areas or re-colonizers of denuded habitats, pre-conditioning the substrates for the later development of other organisms or inhibiting their settlement (Zidarova and others, 2020). In addition, the fact that diatoms are capable of growth in a wide variety of environmental conditions, are tolerant to desiccation and freezing, and the wide types of diatoms found in cryoconite holes suggest multiple origins of colonizing cells (Yallop and Anesio, 2010). According to these authors, cryoconites may act as a reservoir, accumulating a large number of diatom species from a variety of local sources.

An interesting result of our study is the presence in samples of the cyst-like stages of the snow algae *Sanguina* sp. together with the flagellated motile stage of Chlamydomonadales. The cysts of the snow algae *Sanguina* sp. are often found in cryoconite, but they were probably just passively transported by melting from snow, where the whole life cycle takes place, to the holes (Procházková and others, 2021). In addition, it has been shown that blooms of snow algae are often composed of more than one species. Indeed, all 18S rRNA gene phylogenetic studies have revealed a single clade comprising immotile spherical red cysts, and none of the motile, flagellated 'green' species ever formed a single phylogenetic clade together with red spherical cysts from red snow (Leya and others, 2003; Remias and others, 2013). Thus, green, flagellated isolates from red snow field samples often were most likely misinterpreted as having resulted from red spherical cysts or even vice versa (Procházková and others, 2021). It is therefore not possible to morphologically determine if the flagellated stage observed in our samples is simply a different life cycle phase of the cyst-like stage or another species.

To date, only the flagellates of the orange snow algae *Sanguina aurantia* have been described (Raymond and others, 2022), which left the question about the life stage of other Chlamydomonadales still unresolved. In addition, a better understanding of the life stage and morphological variations of these taxa could provide valuable information about their ecology, as flagellates, which are able to reproduce, are much more sensitive to freezing and high irradiation than cysts of the same species (Remias, 2012). Further molecular studies are thus needed to better understand the life cycle and the ecology of these Chlamydomonadales within the cryoconite holes in Antarctica.

In glacial environments, the phenomenon of ice albedo reduction due to algae proliferation is caused by warming but also constitutes a factor aggravating the effects of climate change. It has previously been demonstrated that the presence of pigmented cyanobacterial engineers, along with other factors (organic matter properties, local geology), could participate in influencing the colors of cryoconite on various glaciers (Beutler and others, 2004; Sajjad, 2020; Williamson, 2020). In our study, the morphological distinction between the different morphotypes allowed us to highlight that microalgae and Cyanobacteria could also have the potential to reduce the albedo. In particular, taxa that have red-pigmented morphotypes, such as *Gloeocapsopsis* sp., *Pleurocapsa* sp., *Sanguina* sp., and *Stigonema* sp., are likely susceptible to induce a reduction of the ice albedo.

5. Conclusion

This study is the first biological characterization of cryoconite holes in the area of the Northern Victoria Land. It demonstrates that Antarctic cryoconite holes are highly diversified habitats for Cyanobacteria and microalgae, in terms of biovolume, morphology, and taxonomy. The work highlights the importance of microalgae, such as Chlorophytes and diatoms, in playing a key role in the cryoconite ecosystem and acting as ecosystem engineers together with Cyanobacteria. The detailed description of the species provided in this study and the comparison of their occurrence in the cryoconite holes with the existing literature appear of great importance for helping future works to identify rare or endemic glacial species that could be endangered as a result of climate change. The rapid disappearance of glacial biodiversity due to glacier melting might mean only a few generations could have the opportunity to study these vanishing ecosystems. By the re-dispersion of cryoconite sediment from the holes onto the ice surface due to warm weather, these pigmented photoautotrophs living in cryoconite could have the potential to reduce the albedo of the ice. The results highlight the importance of conducting further studies regrouping biological, geological, chemical, and spectrophotometric data to better understand the role of the photoautotroph component in the albedo reduction in Antarctica.

Antarctica is one of the regions most seriously impacted by climate change (Turner and others, 2009). The primary effects of this regional warming include massive ice losses, as evidenced by glacier retreat, ice shelf collapses, and a decrease in sea ice. The retreat of glaciers is opening up new areas available for colonization and biological succession, referred to as 'newly ice-free areas' (Rückamp and others, 2011; Lagger and others, 2018). The recent predictions forecast that melts across the Antarctic continent will lead to the emergence of between 2100 and 17267 km^2 of new ice-free area by the end of this century (Lee, 2017). As glaciers retreat, the cyanobacterial and microalgae cells residing in cryoconite have the potential to act as seeding agents for newly terrestrial and aquatic habitats in proglacial sites, as it has been suggested by Yallop and Anesio (2010). This phenomenon should be particularly important in the case of high coverage of cryoconite holes on the glacier surface and large hole diameters. This study paves the way for a deeper understanding of the photoautotroph community in cryoconite holes in Antarctica.

Supplementary material. The supplementary material for this article can be found at https://doi.org/10.1017/jog.2025.12.

https://doi.org/10.1017/jog.2025.12 Published online by Cambridge University Press

Data availability statement. All data supporting the findings of this study are available within the paper and its Supplementary Information.

Acknowledgements. We thank K. Kopalová for his help with microalgae determination. We would also like to show our gratitude to the collaborators and students, who have contributed to the collection and analysis of data, and the alpine guides and helicopter pilots of Mario Zucchelli Station (MZS) for having supported the field activities.

Author contributions. Flavia Dory: Conceptualization, Data curation, Formal analysis, Investigation, Methodology, Resources, Visualization, Writing – original draft, Writing – review & editing. Veronica Nava: Validation, Writing – review & editing. Linda Nedbalovà: Validation, Writing – review & editing. Morena Spreafico: Validation, Writing – review & editing. Valentina Soler: Validation, Writing – review & editing. Biagio Di Mauro: Funding acquisition, Resources, review. Giacomo Traversa: Resources, Visualization, review. Barbara Leoni: Conceptualization, Data curation, Formal analysis, Investigation, Methodology, Project administration, Resources, Supervision, Visualization, Writing – original draft, Writing – review & editing.

Funding statement. This study was supported by the project Bio-Geo Albedo feedback at Antarctic Ice-Sheet margins (no. PNRA18_00222) funded by the National Antarctic Research Program of Italy (PNRA).

Competing interests. The authors declare no conflicts of interest.

References

Amalfitano S and Fazi S (2008) Recovery and quantification of bacterial cells associated with streambed sediments. *Journal of Microbiological Methods* **75**(2), 237–243. doi:10.1016/j.mimet.2008.06.004

Anesio AM and Laybourn-Parry J (2012) Glaciers and ice sheets as a biome. *Trends in Ecology and Evolution* **27**(4), 219–225. doi:10.1016/j.tree.2011.09.012

Bagshaw EA, Tranter M, Fountain AG, Welch KA, Basagic H and Lyons WB (2007) Biogeochemical evolution of cryoconite holes on Canada Glacier, Taylor Valley, Antarctica. *Journal of Geophysical Research: Biogeosciences* **112**(G4), G04S35. doi:10.1029/2007JG000442

Bagshaw EA, Tranter M, Fountain AG, Welch K, Basagic HJ and Lyons WB (2013) Do cryoconite holes have the potential to be significant sources of C, N, and P to downstream depauperate ecosystems of Taylor Valley, Antarctica?. *Arctic, Antarctic, and Alpine Research* **45**(4), 440–454. doi:10.1657/1938-4246-45.4.440

Battarbee RW and **6 others** (2001) *Tracking Environmental Change using Lake Sediments*. Diatoms, 155–202. Springer Netherlands. https://eprints.ncl.ac.uk.

Beutler M, Wiltshire KH, Reineke C and Hansen U-P (2004) Algorithms and practical fluorescence models of the photosynthetic apparatus of red cyanobacteria and Cryptophyta designed for the fluorescence detection of red cyanobacteria and cryptophytes. *Aquatic Microbial Ecology* **35**(2), 115–129. doi:10.3354/ame035115

Bishop J (2020) *Ecology and Taxonomy of limno-terrestrial diatoms from East Antarctica*. PhD thesis supervised by Kopalová, Kateřina. Prague: Charles University, Faculty of Science, Department of Ecology.

Boetius A, Anesio AM, Deming JW, Mikucki JA and Rapp JZ (2015) Microbial ecology of the cryosphere: Sea ice and glacial habitats. *Nature Reviews, Microbiology* **13**(11), 677–690. doi:10.1038/nrmicro3522

Bøggild CE, Brandt RE, Brown KJ and Warren SG (2010) The ablation zone in northeast Greenland: Ice types, albedos and impurities. *Journal of Glaciology* **56**(195), 101–113. doi:10.3189/002214310791190776

Borchhardt N and **6 others** (2017) Diversity of algae and lichens in biological soil crusts of Ardley and King George islands, Antarctica. *Antarctic Science* **29**(3), 229–237. doi:10.1017/S0954102016000638

Borics G, Abonyi A, Salmaso N and Ptacnik R (2021) Freshwater phytoplankton diversity: Models, drivers and implications for ecosystem properties. *Hydrobiologia* **848**(1), 53–75. doi:10.1007/s10750-020-04332-9

Broady P (2005) The distribution of terrestrial and hydro-terrestrial algal associations at three contrasting locations in southern Victoria Land, Antarctica. *Algological Studies* **118**, 95–112. doi:10.1127/1864-1318/2006/0118-0095

Broady PA and Kibblewhite AL (1991) Morphological characterization of Oscillatoriales (Cyanobacteria) from Ross Island and southern Victoria Land, Antarctica. *Antarctic Science* **3**(1), 35–45. doi:10.1017/S095410209100007X

Buda J and **12 others** (2020) Biotope and biocenosis of cryoconite hole ecosystems on Ecology Glacier in the maritime Antarctic. *Science of the Total Environment* **724**, 138112. doi:10.1016/j.scitotenv.2020.138112

Budgeon AL, Roberts D, Gasparon M and Adams N (2012) Direct evidence of aeolian deposition of marine diatoms to an ice sheet. *Antarctic Science* **24**(5), 527–535. doi:10.1017/S0954102012000235

Cameron KA, Hodson AJ and Osborn AM (2012) Structure and diversity of bacterial, eukaryotic and archaeal communities in glacial cryoconite holes from the Arctic and the Antarctic. *FEMS Microbiology Ecology* **82**(2), 254–267. doi:10.1111/j.1574-6941.2011.01277.x

Christner BC, Kvitko BH and Reeve JN (2003) Molecular identification of Bacteria and Eukarya inhabiting an Antarctic cryoconite hole. *Extremophiles* **7**(3), 177–183. doi:10.1007/s00792-002-0309-0

Clarke KR and Warwick RM (1994) Similarity-based testing for community pattern: The two-way layout with no replication. *Marine Biology* **118**(1), 167–176. doi:10.1007/BF00699231

Cook J, Edwards A, Takeuchi N and Irvine-Fynn T (2016) Cryoconite: The dark biological secret of the cryosphere. *Progress in Physical Geography: Earth and Environment* **40**(1), 66–111. doi:10.1177/0309133315616574

Cook JM and **7 others** (2012) An improved estimate of microbially mediated carbon fluxes from the Greenland ice sheet. *Journal of Glaciology* **58**(212), 1098–1108. doi:10.3189/2012JoG12J001

Cook JM, Hodson AJ, Taggart AJ, Mernild SH and Tranter M (2017) A predictive model for the spectral "bioalbedo" of snow. *Journal of Geophysical Research: Earth Surface* **122**(1), 434–454. doi:10.1002/2016JF003932

Cremer H, Gore D, Hultzsch N, Melles M and Wagner B (2004) The diatom flora and limnology of lakes in the Amery Oasis, East Antarctica. *Polar Biology* **27**(9), 513–531. doi:10.1007/s00300-004-0624-2

Das SK and Singh D (2021) Epiphytic Algae on the Bryophytes of Larsemann Hills, East Antarctica. *National Academy Science Letters* **44**(2), 161–165. doi:10.1007/s40009-020-00947-7

Di Mauro B and **7 others** (2017) Impact of impurities and cryoconite on the optical properties of the Morteratsch Glacier (Swiss Alps). *The Cryosphere* **11**(6), 2393–2409. doi:10.5194/tc-11-2393-2017

Di Mauro B and **8 others** (2020) Glacier algae foster ice-albedo feedback in the European Alps. *Scientific Reports* **10**(1), 4739. doi:10.1038/s41598-020-61762-0

Di Mauro B and **9 others** (2024) Combined effect of algae and dust on snow spectral and broadband albedo. *Journal of Quantitative Spectroscopy and Radiative Transfer* **316**, 108906. doi:10.1016/j.jqsrt.2024.108906

Druart J-C and Rimet F (2008) Protocoles d'analyse du phytoplancton de l'INRA: Prélèvement, dénombrement et biovolumes (report). *INRA-Thonon, Rapport SHL 283*, 96.

Edwards A and **7 others** (2013) A metagenomic snapshot of taxonomic and functional diversity in an alpine glacier cryoconite ecosystem. *Environmental Research Letters* **8**(3), 035003. doi:10.1088/1748-9326/8/3/035003

Ettl H and Gärtner G (1999) *Süßwasserflora von Mitteleuropa, Bd. 10: Chlorophyta II*. Stuttgart, Germany; New York, NY, USA: *Tetrasporales, Chlorococcales, Gloeodendrales*; Gustav Fischer Verlag. https://link.springer.com/book/9783827421258.

Fernández-Carazo R, Namsaraev Z, Mano M-J, Ertz D and Wilmotte A (2012) Cyanobacterial diversity for an anthropogenic impact assessment in the Sør Rondane Mountains area, Antarctica. *Antarctic Science* **24**(3), 229–242. doi:10.1017/S0954102011000824

Fountain AG, Tranter M, Nylen TH, Lewis KJ and Mueller DR (2004) Evolution of cryoconite holes and their contribution to meltwater runoff from glaciers in the McMurdo Dry Valleys, Antarctica. *Journal of Glaciology* **50**(168), 35–45. doi:10.3189/172756504781830312

Hindák F (2008) *Colour Atlas of Cyanophytes*. VEDA, Publishing House of the Slovak Academy of Sciences: Bratislava, Czecho-Slovakia.

Hodson A and **10 others** (2007) A glacier respires: Quantifying the distribution and respiration CO2 flux of cryoconite across an entire Arctic supraglacial

ecosystem. *Journal of Geophysical Research: Biogeosciences* **112**(G4), G04S36. doi:10.1029/2007JG000452

Hodson A and **7 others** (2008) Glacial Ecosystems. *Ecological Monographs* **78**(1), 41–67. doi:10.1890/07-0187.1

Hodson A and **6 others** (2010) The cryoconite ecosystem on the Greenland ice sheet. *Annals of Glaciology* **51**(56), 123–129. doi:10.3189/172756411795931985

Hodson A, Paterson H, Westwood K, Cameron K and Laybourn-Parry J (2013) A blue-ice ecosystem on the margins of the East Antarctic ice sheet. *Journal of Glaciology* **59**(214), 255–268. doi:10.3189/2013JoG12J052

Hotaling S and **10 others** (2021) Biological albedo reduction on ice sheets, glaciers, and snowfields. *Earth-Science Reviews* **220**, 103728. doi:10.1016/j.earscirev.2021.103728

Jackson EE, Hawes I and Jungblut AD (2021) 16S rRNA gene and 18S rRNA gene diversity in microbial mat communities in meltwater ponds on the McMurdo Ice Shelf, Antarctica. *Polar Biology* **44**(4), 823–836. doi:10.1007/s00300-021-02843-2

Jeon M and **9 others** (2021) Phytoplankton succession during a massive coastal diatom bloom at Marian Cove, King George Island, Antarctica. *Polar Biology* **44**(10), 1993–2010. doi:10.1007/s00300-021-02933-1

Johansen J and **6 others** (2017) A revision of the genus *Geitlerinema* and a description of the genus *Anagnostidinema* gen. nov. (Oscillatoriophycidae, Cyanobacteria). *Fottea. Faculty Bibliography*, 40. https://collected.jcu.edu/fac_bib_2017/40.

Jungblut A-D and **6 others** (2005) Diversity within cyanobacterial mat communities in variable salinity meltwater ponds of McMurdo Ice Shelf, Antarctica. *Environmental Microbiology* **7**(4), 519–529. doi:10.1111/j.1462-2920.2005.00717.x

Jungblut A-D and **8 others** (2016) Microbial mat communities along an oxygen gradient in a perennially ice-covered Antarctic Lake. *Applied and Environmental Microbiology* **82**(2), 620–630. doi:10.1128/AEM.02699-15

Jungblut AD and Vincent WF (2017) Cyanobacteria in polar and alpine ecosystems. In Margesin R (ed), *Psychrophiles: From Biodiversity to Biotechnology*. Cham: Springer International Publishing, 181–206.

Kaczmarek Ł, Jakubowska N, Celewicz-Gołdyn S and Zawierucha K (2016) The microorganisms of cryoconite holes (algae, Archaea, bacteria, cyanobacteria, fungi, and Protista): A review. *Polar Record* **52**(2), 176–203. doi:10.1017/S0032247415000637

Kaštovská K, Elster J, Stibal M and Šantrůčková H (2005) Microbial assemblages in soil microbial succession after glacial retreat in Svalbard (high Arctic). *Microbial Ecology* **50**(3), 396–407. doi:10.1007/s00248-005-0246-4

Kohler T, Kopalová K, Van de Vijver B and Kociolek P (2015) The genus *Luticola* D.G.Mann (Bacillariophyta) from the McMurdo Sound Region, Antarctica, with the description of four new species. *Phytotaxa* **208**, 103. doi:10.11646/phytotaxa.208.2.1

Komárek J (1999) Diversity of cyanoprokaryotes (cyanobacteria) of King George Island, maritime Antarctica-a survey. *Algological Studies/Archiv Für Hydrobiologie, Supplement Volumes* **129**, 181–193. doi:10.1127/algol_stud/94/1999/181

Komárek J (2014) Phenotypic and ecological diversity of freshwater coccoid cyanobacteria from maritime Antarctica and Islands of NW Weddell Sea. II. *Czech Polar Reports* **4**(1), 17–39. doi:10.5817/CPR2014-1-3

Komárek J, and Anagnostidis K (2005) *Süßwasserflora von Mitteleuropa: Cyanoprokaryota*. Berlin Heidelberg: Spektrum, Akad. Verlag.

Komárek J and Elster J (2008) Ecological background of cyanobacterial assemblages of the northern part of James Ross Island, Antarctica. *Polish Polar Research* **29**(1), 17–32.

Komárek J, Genuário DB, Fiore MF and Elster J (2015) Heterocytous cyanobacteria of the Ulu Peninsula, James Ross Island, Antarctica. *Polar Biology* **38**(4), 475–492. doi:10.1007/s00300-014-1609-4

Komárek O and Komárek J (2010) Diversity and ecology of cyanobacterial microflora of Antarctic seepage habitats: Comparison of King George Island, Shetland Islands, and James Ross Island, NW Weddell Sea, Antarctica. In Seckbach J and Oren A (eds), *Microbial Mats: Modern and Ancient Microorganisms in Stratified Systems*. Dordrecht: Springer Netherlands, 515–539.

Kopalová K, Elster J, Nedbalová L and Van De Vijver B (2009) Three new terrestrial diatom species from seepage areas on James Ross Island (Antarctic Peninsula Region). *Diatom Research* **24**(1), 113–122. doi:10.1080/0269249X.2009.9705786

Kopalová K, Nedbalová L, de Haan M and Van de Vijver B (2011) Description of five new species of the diatom genus *Luticola* (Bacillariophyta, Diadesmidaceae) found in lakes of James Ross Island (Maritime Antarctic Region). *Phytotaxa* **27**, 44–60. doi:10.11646/phytotaxa.27.1.5

Lagger C, Nime M, Torre L, Servetto N, Tatián M and Sahade R (2018) Climate change, glacier retreat and a new ice-free island offer new insights on Antarctic benthic responses. *Ecography* **41**(4), 579–591. doi:10.1111/ecog.03018

Lange-Bertalot H, Hofmann GM, Werum M, and Cantonati M (2017) Freshwater Benthic Diatoms of Central Europe. Over 800 common species used in ecological assessment. *English Edition with Updated Taxonomy and Added Species* Cantonati M, Kelly MG, Lange-Bertalot H (eds), 1–942. Schmitten-Oberreifenberg: Koeltz Botanical Books.

Langford H, Hodson A, Banwart S and Bøggild C (2010) The microstructure and biogeochemistry of Arctic cryoconite granules. *Annals of Glaciology* **51**(56), 87–94. doi:10.3189/172756411795932083

Laplace-Treyture C, Derot J, Prévost E, Le Mat A and Jamoneau A (2021) Phytoplankton morpho-functional trait dataset from French water-bodies. *Scientific Data* **8**(1), 40. doi:10.1038/s41597-021-00814-0

Lee JR and **6 others** (2017) Climate change drives expansion of Antarctic ice-free habitat. *Nature* **547**(7661), 49–54. doi:10.1038/nature22996

Legendre P and Legendre L (1998) Numerical ecology: Developments in environmental modelling. *Developments in Environmental Modelling*, Vol. 20(1), 2nd. Amsterdam: Elsevier.

Levkov Z (2016) Species of the diatom genus *Craticula* Grunow (Bacillariophyceae) from Macedonia. *Contributions, Section of Natural, Mathematical and Biotechnical Sciences, MASA* **37**, 129–165. doi:10.20903/CSNMBS_MASA.2016.37.2.40

Leya T, Müller T, Ling HU, and Fuhr G (2003) Snow algae from north-western Spitsbergen (Svalbard). *The coastal ecosystem of Kongsfjorden, Svalbard Synopsis of biological research performed at the Koldewey Station in the years 1991*. https://core.ac.uk/download/pdf/11769644.pdf#page=52.

Lizieri C, Schaefer CEGR and Hawes I (2022) Morphological diversity of benthic cyanobacterial assemblages in meltwater ponds along environmental gradients in the McMurdo Sound region, Antarctica. *Anais da Academia Brasileira de Ciências* **94**, e20210814. doi:10.1590/0001-3765202220210814

Luo W and **7 others** (2020) Molecular diversity of the microbial community in coloured snow from the Fildes Peninsula (King George Island, Maritime Antarctica). *Polar Biology* **43**(9), 1391–1405. doi:10.1007/s00300-020-02716-0

Mataloni G and Komárek J (2004) *Gloeocapsopsis aurea*, a new subaerophytic cyanobacterium from maritime Antarctica. *Polar Biology* **27**(10), 623–628. doi:10.1007/s00300-004-0620-6

Mataloni G, Tell G and Wynn-Williams DD (2000) Structure and diversity of soil algal communities from Cierva Point (Antarctic Peninsula). *Polar Biology* **23**(3), 205–211. doi:10.1007/s003000050028

Mikhailyuk T, Glaser K, Holzinger A and Karsten U (2015) Biodiversity of *Klebsormidium* (Streptophyta) from alpine biological soil crusts (Alps, Tyrol, Austria, and Italy). *Journal of Phycology* **51**(4), 750–767. doi:10.1111/jpy.12316

Millar JL, Bagshaw EA, Edwards A, Poniecka EA and Jungblut AD (2021) Polar cryoconite associated microbiota is dominated by hemispheric specialist genera. *Frontiers in Microbiology* **12**, 738451. doi:10.3389/fmicb.2021.738451

Mueller DR and Pollard WH (2004) Gradient analysis of cryoconite ecosystems from two polar glaciers. *Polar Biology* **27**(2), 66–74. doi:10.1007/s00300-003-0580-2

Mueller D, Warwick V, Wayne P and Fritsen C (2001) Glacial cryoconite ecosystems: A bipolar comparison of algal communities and habitats. *Nova Hedwigia Beiheft* **123**, 173.

Nienaber MA, and Steinitz-Kannan M (2018) *A Guide to Cyanobacteria: Identification and Impact*. Lexington, KY, USA: University Press of Kentucky.

Ohtani S and Kanda H (1987) Epiphytic algae on the moss community of *Grimmia Lawiana* around Syowa Station, Antarctica (Ninth Symposium

on Polar Biology). *Proceedings of the NIPR Symposium on Polar Biology* **1**, 255–264.

Oksanen J (2010) Package 'vegan.' *Community Ecology Package, Version*. **2**(9), 1–295.

Pandey KD and **6 others** (2004) Cyanobacteria in Antarctica: Ecology, physiology and cold adaptation. *Cellular and Molecular Biology* **50**(5), 575–584.

Pinseel E, Van de Vijver B and Kopalova K (2015) *Achnanthidium petuniabuktianum* sp. nov. (Achnanthidiaceae, Bacillariophyta), a new representative of the *A. pyrenaicum* group from Spitsbergen (Svalbard Archipelago, High Arctic). *Phytotaxa* **226**(1), 63. doi:10.11646/phytotaxa.226.1.6

Porazinska DL, Fountain AG, Nylen TH, Tranter M, Virginia RA and Wall DH (2004) The Biodiversity and Biogeochemistry of Cryoconite Holes from McMurdo Dry Valley Glaciers, Antarctica. *Arctic, Antarctic, and Alpine Research* **36**(1), 84–91. doi:10.1657/1523-0430(2004)036[0084:TBABOC]2.0.CO;2

Procházková L, Leya T, Křížková H and Nedbalová L (2019) *Sanguina nivaloides* and *Sanguina aurantia* gen. et spp. nov. (Chlorophyta): The taxonomy, phylogeny, biogeography and ecology of two newly recognised algae causing red and Orange snow. *FEMS Microbiology Ecology* **95**(6), fiz064. doi:10.1093/femsec/fiz064

Procházková L, Remias D, Holzinger A, Řezanka T and Nedbalová L (2021) Ecophysiological and ultrastructural characterisation of the circumpolar Orange snow alga Sanguina aurantia compared to the cosmopolitan red snow alga *Sanguina nivaloides* (Chlorophyta). *Polar Biology* **44**(1), 105–117. doi:10.1007/s00300-020-02778-0

Raymond BB, Engstrom CB and Quarmby LM (2022) The underlying green biciliate morphology of the Orange snow alga *Sanguina aurantia*. *Current Biology* **32**(2), R68–R69. doi:10.1016/j.cub.2021.12.005

R Development Core Team (2018) R: A language and environment for statistical computing; 2018.

Remias D (2012) Cell structure and physiology of alpine snow and ice algae. In Lütz C ((ed)), *Plants in Alpine Regions: Cell Physiology of Adaption and Survival Strategies*. Vienna: Springer, 175–185.

Remias D, Wastian H, Lütz C and Leya T (2013) Insights into the biology and phylogeny of *Chloromonas polyptera* (Chlorophyta), an alga causing Orange snow in Maritime Antarctica. *Antarctic Science* **25**(5), 648–656. doi:10.1017/S0954102013000060

Rippin M, Borchhardt N, Karsten U and Becker B (2019) Cold acclimation improves the desiccation stress resilience of polar strains of *Klebsormidium* (Streptophyta). *Frontiers in Microbiology* **10**, 1730. doi:10.3389/fmicb.2019.01730

Rosen BH and Amand AS (2015) *Field and laboratory guide to freshwater cyanobacteria harmful algal blooms for Native American and Alaska Native communities*. 2015–1164. U.S. Geological Survey. doi:10.3133/ofr20151164.

Rozwalak P and **32 others** (2022) Cryoconite – From minerals and organic matter to bioengineered sediments on glacier's surfaces. *Science of the Total Environment* **807**, 150874. doi:10.1016/j.scitotenv.2021.150874

Rückamp M, Braun M, Suckro S and Blindow N (2011) Observed glacial changes on the King George Island ice cap, Antarctica, in the last decade. *Global and Planetary Change* **79**(1), 99–109. doi:10.1016/j.gloplacha.2011.06.009

Rybalka N and **9 others** (2023) Unrecognized diversity and distribution of soil algae from Maritime Antarctica (Fildes Peninsula, King George Island). *Frontiers in Microbiology*, 14. doi:10.3389/fmicb.2023.1118747

Sabbe K, Verleyen E, Hodgson DA, Vanhoutte K and Vyverman W (2003) Benthic diatom flora of freshwater and saline lakes in the Larsemann Hills and Rauer Islands, East Antarctica. *Antarctic Science* **15**(2), 227–248. doi:10.1017/S095410200300124X

Sajjad W and **7 others** (2020) Pigment production by cold-adapted bacteria and fungi: Colorful tale of cryosphere with wide range applications. *Extremophiles* **24**(4), 447–473. doi:10.1007/s00792-020-01180-2

Segawa T and **9 others** (2017) Biogeography of cryoconite forming cyanobacteria on polar and Asian glaciers. *Journal of Biogeography* **44**(12), 2849–2861. doi:10.1111/jbi.13089

Shalygin S and **4 others** (2019) Neotypification of *Pleurocapsa fuliginosa* and epitypification of *P. minor* (Pleurocapsales): Resolving a polyphyletic cyanobacterial genus. *Phytotaxa* **392**(4), 245. doi:10.11646/phytotaxa.392.4.1

Sommers P and **6 others** (2018) Diversity patterns of microbial eukaryotes mirror those of bacteria in Antarctic cryoconite holes. *FEMS Microbiology Ecology* **94**(1), fix167. doi:10.1093/femsec/fix167

Spaulding SA, McKnight DM, Stoermer EF and Doran PT (1997) Diatoms in sediments of perennially ice-covered Lake Hoare, and implications for interpreting lake history in the McMurdo Dry Valleys of Antarctica. *Journal of Paleolimnology* **17**(4), 403–420. doi:10.1023/A:1007931329881

Stanish LF, Bagshaw EA, McKnight DM, Fountain AG and Tranter M (2013) Environmental factors influencing diatom communities in Antarctic cryoconite holes. *Environmental Research Letters* **8**(4), 045006. doi:10.1088/1748-9326/8/4/045006

Stibal M, Šabacká M and Kaštovská K (2006) Microbial communities on glacier surfaces in Svalbard: impact of physical and chemical properties on abundance and structure of cyanobacteria and algae. *Microbial Ecology* **52**(4), 644–654. doi:10.1007/s00248-006-9083-3

Takeuchi N and **6 others** (2018) Temporal variations of cryoconite holes and cryoconite coverage on the ablation ice surface of Qaanaaq Glacier in northwest Greenland. *Annals of Glaciology* **59**(77), 21–30. doi:10.1017/aog.2018.19

Takeuchi N, Kohshima S and Seko K (2001) Structure, formation, and darkening process of Albedo-Reducing Material (Cryoconite) on a Himalayan Glacier: A Granular Algal Mat Growing on the Glacier. *Arctic, Antarctic, and Alpine Research* **33**(2), 115–122. doi:10.2307/1552211

Taton A, Grubisic S, Balthasart P, Hodgson DA, Laybourn-Parry J and Wilmotte A (2006) Biogeographical distribution and ecological ranges of benthic cyanobacteria in East Antarctic lakes. *FEMS Microbiology Ecology* **57**(2), 272–289. doi:10.1111/j.1574-6941.2006.00110.x

Tranter M and **others** (2004) Extreme hydrochemical conditions in natural microcosms entombed within Antarctic ice. *Hydrological Processes* **18**(2), 379–387. doi:10.1002/hyp.5217

Traversa G, Scipinotti R, Pierattini S, Fasani B, and Di Mauro B (2024) Cryoconite holes geomorphometry, spatial distribution and radiative impact over the Hells Gate Ice Shelf (East Antarctica). *Annals of Glaciology* **65**, e22. doi:10.1017/aog.2024.20

Turner J and **8 others** (2009) *Antarctic Climate Change and the Environment*. Published by the Scientific Committee on Antarctic Research Scott Polar Research Institute, Lensfield Road, Cambridge, UK. ISBN 978-0-948277-22-1. https://epic.awi.de/id/eprint/21227/1/Tur2009a.pdf.

Utermöhl H (1958) Methods of collecting plankton for various purposes are discussed. Zur Vervollkommnung der quantitativen Phytoplankton-Methodik. *Internationale Vereinigung Für Theoretische Und Angewandte Limnologie: Mitteilungen* **9**(1), 1–38. doi:10.1080/05384680.1958.11904091

Valdespino-Castillo PM and **7 others** (2018) Microbial distribution and turnover in Antarctic microbial mats highlight the relevance of heterotrophic bacteria in low-nutrient environments. *FEMS Microbiology Ecology* **94**(9), fiy129. doi:10.1093/femsec/fiy129

Valdivia N, Garrido I, Bruning P, Piñones A and Pardo LM (2020) Biodiversity of an Antarctic rocky subtidal community and its relationship with glacier meltdown processes. *Marine Environmental Research* **159**, 104991. doi:10.1016/j.marenvres.2020.104991

Van de Vijver B and **8 others** (2010) Four new non-marine diatom taxa from the Subantarctic and Antarctic Regions. *Diatom Research* **25**(2), 431–443. doi:10.1080/0269249X.2010.9705861

Van de Vijver B, Kateřina K and Zidarova R (2015) Three new *Craticula* species (Bacillariophyta) from the Maritime Antarctic Region. *Phytotaxa* **213**, 35–45. doi:10.11646/phytotaxa.213.1.3

Van de Vijver B, Kopalová K and Zidarova R (2016) Revision of the *Psammothidium germainii* complex (Bacillariophyta) in the Maritime Antarctic Region. *Fottea* **16**(2), 145–156. doi:10.5507/fot.2016.008

Van de Vijver B, Zidarova R and de Haan M (2011) Four new *Luticola* taxa (Bacillariophyta) from the South Shetland Islands and James Ross Island (Maritime Antarctic Region). *Nova Hedwigia* **92**, 137–158. doi:10.1127/0029-5035/2011/0092-0137

Velichko N, Smirnova S, Averina S and Pinevich A (2021) A survey of Antarctic cyanobacteria. *Hydrobiologia* **848**(11), 2627–2652. doi:10.1007/s10750-021-04588-9

Vyverman W and **9 others** (2010) Evidence for widespread endemism among Antarctic micro-organisms. *Polar Science* **4**(2), 103–113. doi:10.1016/j.polar.2010.03.006

Weisleitner K, Perras AK, Unterberger SH, Moissl-Eichinger C, Andersen DT and Sattler B (2020) Cryoconite hole location in east-Antarctic Untersee Oasis shapes physical and biological diversity. *Frontiers in Microbiology*, 11. doi:10.3389/fmicb.2020.01165

Wejnerowski Ł and **8 others** (2023) Empirical testing of cryoconite granulation: Role of cyanobacteria in the formation of key biogenic structure darkening glaciers in polar regions. *Journal of Phycology* **59**(5), 939–949. doi:10.1111/jpy.13372

Wharton RA, Vinyard WC, Parker BC, Simmons GM and Seaburg KG, Jr (1981) Algae in cryoconite holes on Canada Glacier in Southern Victorialand, Antarctica. *Phycologia*. doi:10.2216/i0031-8884-20-2-208.1

Williamson CJ and **11 others** (2020) Algal photophysiology drives darkening and melt of the Greenland Ice Sheet. *Proceedings of the National Academy of Sciences* **117**(11), 5694–5705. doi:10.1073/pnas.1918412117

Yakushev AV and **7 others** (2022) Organization of microbial communities in soils: experiment with fouling glasses in extreme terrestrial landscapes of Antarctica. *Eurasian Soil Science* **55**(12), 1770–1785. doi:10.1134/S1064229322700089

Yallop ML and Anesio AM (2010) Benthic diatom flora in supraglacial habitats: A generic-level comparison. *Annals of Glaciology* **51**(56), 15–22. doi:10.3189/172756411795932029

Zawierucha K and **6 others** (2022) Trophic and symbiotic links between obligate-glacier water bears (Tardigrada) and cryoconite microorganisms. *PLoS One* **17**(1), e0262039. doi:10.1371/journal.pone.0262039

Zębek E, Napiórkowska-Krzebietke A, Świątecki A and Górniak D (2021) Biodiversity of periphytic cyanobacteria and algae assemblages in polar region: A case study of the vicinity of Arctowski Polish Antarctic Station (King George Island, Antarctica). *Biodiversity and Conservation* **30**(10), 2751–2771. doi:10.1007/s10531-021-02219-2

Zhang L, Jungblut AD, Hawes I, Andersen DT, Sumner DY and Mackey TJ (2015) Cyanobacterial diversity in benthic mats of the McMurdo Dry Valley lakes, Antarctica. *Polar Biology* **38**(8), 1097–1110. doi:10.1007/s00300-015-1669-0

Zidarova R (2008) Algae from Livingston Island (S Shetland Islands): A checklist. *Phytologia Balcanica* **14**, 19–35.

Zidarova R, Ivanov P and Dzhembekova N (2020) Diatom colonization and community development in Antarctic marine waters – A short-term experiment. *Polish Polar Research* **41**(2), 187–212. doi:10.24425/ppr.2020.133012

Zidarova R, Kopalová K and Van de Vijver B (2016b) Ten new Bacillariophyta species from James Ross Island and the South Shetland Islands (Maritime Antarctic Region). *Phytotaxa* **272**(1), 37–62. doi:10.11646/phytotaxa.272.1.2

Zidarova R, Kopalová K, Van de Vijver B and Lange-Bertalot H (2016a) *Diatoms from the Antarctic Region, Maritime Antarctica* (ISBN: 978-3-946583-05-9). https://repository.uantwerpen.be/link/irua/140969.

https://doi.org/10.1017/jog.2025.12 Published online by Cambridge University Press